GEOLOGICAL SURVEY OF CANADA
OPEN FILE 6968

EXTECH IV Mineralogical Database: XRD, Infrared and TEM Analyses

J.B. Percival, T. Jensen, K. Wasyliuk, G. Drever, J. Sader,
M. Sarfi, P.A. Hunt, C. Bibby, S. Wong, and A. Enright

2012

Natural Resources Canada | Ressources naturelles Canada

Canada

GEOLOGICAL SURVEY OF CANADA
OPEN FILE 6968

EXTECH IV Mineralogical Database: XRD, Infrared and TEM Analyses

J.B. Percival, T. Jensen, K. Wasyliuk, G. Drever, J. Sader, M. Sarfi, P.A. Hunt, C. Bibby, S. Wong, and A. Enright

2012

doi: 10.4095/292112

This publication is available for free download through GEOSCAN (http://geoscan.ess.nrcan.gc.ca/).

Recommended citation

Percival, J.B., Jensen, T., Wasyliuk, K., Drever, G., Sader, J., Sarfi, M., Hunt, P.A., Bibby, C. Wong, S., and Enright, A., 2012. EXTECH IV Mineralogical Database: XRD, Infrared and TEM Analyses; Geological Survey of Canada, Open File 6968, 39 p. doi: 10.4095/292112

Publications in this series have not been edited; they are released as submitted by the author.

EXTECH IV MINERALOGY DATABASE: XRD, INFRARED and TEM ANALYSES

Percival, J.B.[1], Jensen, T.[2*], Wasyliuk, K.[3] , Drever, G.[4], Sader, J.[5*], Sarfi, M.[6*], Hunt, P.A.[1], Bibby, C.[7] Wong, S.[8▪] and Enright, A.[9▪]

[1] Geological Survey of Canada, 601 Booth Street, Ottawa, Ontario K1A 0E8
[2] Senior Environmental Advisor, Senex Energy Limited, 144 Edward Street, Level 11, Brisbane, Queensland, Australia 4001
[3] Cameco Corporation, 2121 11th St. W., Saskatoon, Saskatchewan S7M 1J3; Currently JNR Resources Inc., PO Box 26061, Saskatoon, Saskatchewan S7K 7H9
[4] Cameco Corporation, 2121 11th St. W., Saskatoon, Saskatchewan S7M 1J3; Currently Vice President, Raven Minerals Corp., Suite 806, 390 Bay Street, Toronto, Ontario M5H 2Y2
[5] Consultant, MMG (Minerals & Metals Group), 999 Canada Place, Vancouver, British Colombia V6C 3E1
[6] Senior Consultant, Environmental Management, Stantec Consulting Inc., 4370 Dominion St. 5th Fl., Burnaby, British Colombia V5G 4L7
[7] CanmetMATERIALS, 183 Longwood Road south, Hamilton, Ontario L8P 0A5
[8] Department of Environmental Sciences, Carleton University, Ottawa, Ontario K1S 5B4
[9] Department of Geology, University of Ottawa, Ottawa, Ontario K1N 6N5 Currently at Department of Earth Sciences, University of Toronto, Toronto, Ontario M5S 3B1
* Former name Reif (see Percival et al., 2002)
▪ Former students

Table of Contents

List of Figures

List of Tables

1. INTRODUCTION

Between 2000 and 2004, the Geological Survey of Canada undertook, with multiple industry, government and university partners and collaborators, a detailed study of the Athabasca Basin in Saskatchewan and Alberta to improve understanding of the basin and its uranium (U) deposits, and to develop new technologies for exploration, particularly at depth. EXTECH (Exploration TECHnology) IV - Athabasca Uranium Multidisciplinary Study, was an integrated partnership between Cameco Corporation, Cogema Resources Inc. (now AREVA Resources Canada Inc.), the universities of Alberta, Laurentian, Regina and Saskatchewan, the geological surveys of Saskatchewan, Alberta and Canada and NSERC (Jefferson and Delaney, 2001). The Project was subdivided into 7 Subprojects with a scientific research team of about 80 individuals, together addressing most aspects of geology, geophysics and geochemistry as summarised in Jefferson and Delaney (2007).

This report forms part of Subproject 7 on Clay Mineral Studies. The objective of this Subproject was to enhance the interpretation of stratigraphy (Subproject 4), diagenesis, and ore deposition, thereby assisting exploration and formulation of a genetic model for these deposits. Clay minerals are a major component of the sandstones and alteration haloes surrounding these world-class unconformity-type U deposits. The deposit genesis can be related to several processes including paleo-weathering, sedimentation, diagenesis and hydrothermal alteration. Clay minerals are sensitive indicators of low temperature environments (Keller, 1970; Hoeve and Quirt, 1984) as their composition, structure and crystallinity are controlled by temperature, fluid chemistry and fluid flux. Valuable information regarding diagenetic and hydrothermal conditions and depth of burial can be ascertained by understanding their nature and extent of alteration (Kisch, 1983; Percival et al., 1993).

This report presents a database of all results from mineralogical analyses carried out between 2000 and 2004 on samples collected from boreholes from Close Lake, McArthur River and Read Lake sites in the McArthur River uranium mine camp. Most of this work was done *in situ* on cached drill core, using a portable infrared spectrometer but some data were obtained in the laboratory of the Geological Survey of Canada using X-ray diffraction (XRD) analyses.

2. GEOLOGICAL SETTING

The McArthur River mine is located within the southeastern Athabasca Basin in northern Saskatchewan (Fig 1). This basin is one of the most important repositories for uranium deposits in the world with respect to size, grade and production. Other analogous metallogenic provinces include the Thelon Basin of Nunavut Territory and the Pine Creek Geosyncline of Northern Territory, Australia. The common denominator of these deposits is their association with unconformities beneath Late Paleoproterozoic siliciclastic basins.

The Athabasca Basin in northern Saskatchewan and Alberta comprises a 100,000 km^2, 2300 m + thick succession (Sibbald, 1985; Ramaekers et al., 2007; Percival et al., 2009) of fluvial sandstone, conglomerate, mudstone and an uppermost carbonate unit of the Athabasca Group.

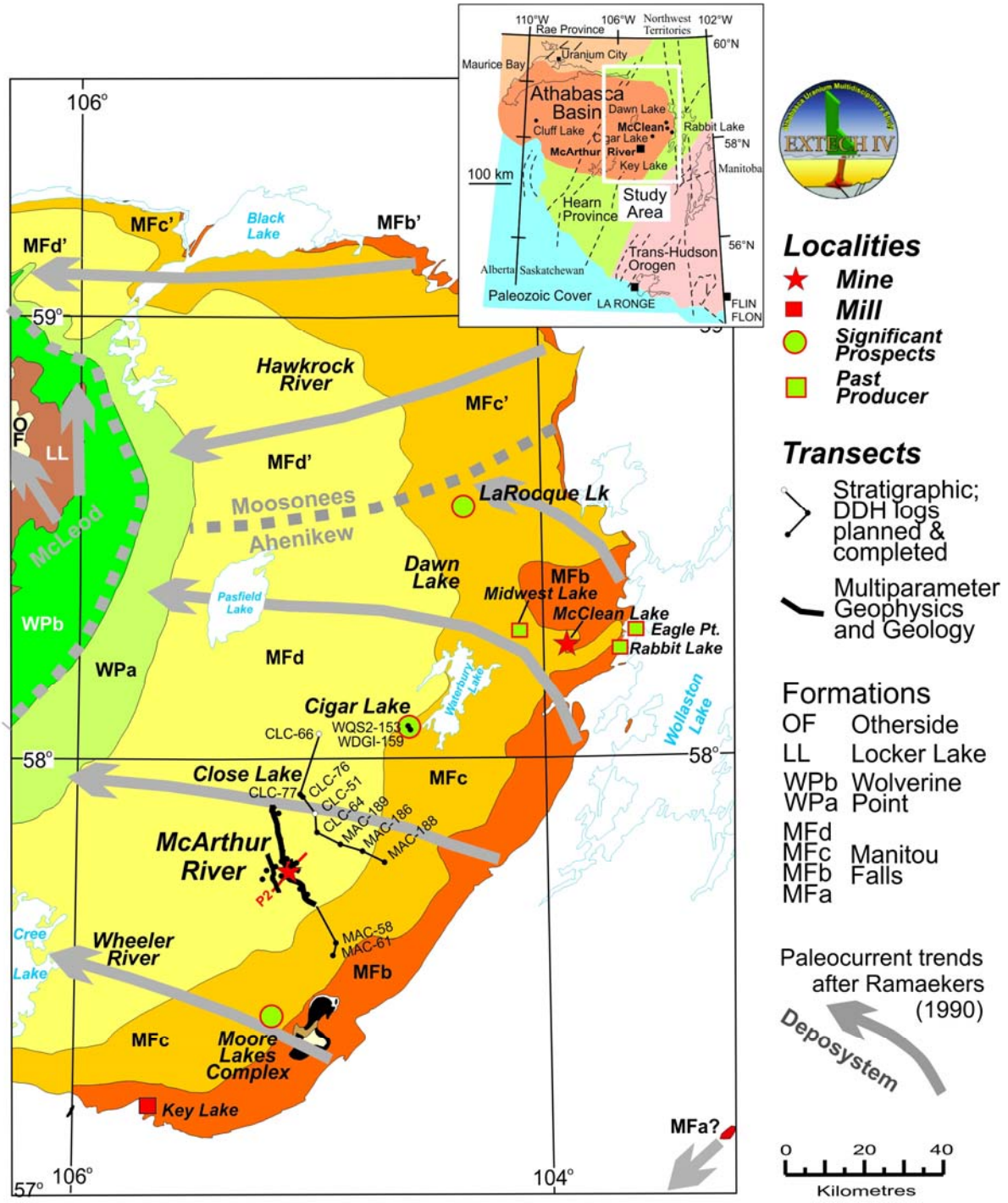

Figure 1. General geology map of the eastern Athabasca Basin showing location of the McArthur River mine relative to other mine camps (after Jefferson et al., 2001). Drill holes logged are shown in grey. Generalized paleocurrents and deposystems based on Ramaekers (1990) and Ramaekers et al. (2007).

Ramaekers et al. (2007) subdivided the Athabasca Group into 4 major sequences, each separated by basin-wide unconformities and with independent paleocurrent and isopach patterns. The McArthur River deposit straddles the basal unconformity, residing mainly with the graphite schist of the P2 fault. The upper part of the deposit is in conglomerate and sandstone at the base of Sequence 2, which here comprises the Read and Manitou Falls formations. The basement rocks are part of the Wollaston Supergroup in the western Churchill Province (Yeo and Delaney, 2007). The Read Formation at McArthur River is the former Manitou Falls A Formation of Ramaekers (1979, 1980, 1981, 1983) and Sibbald (1985).

The lowermost unit, the Read Formation, consists of red silty mudstone, quartz pebble conglomerate and quartz arenite. According to Yeo et al. (2007) the formation represents flashy braided stream, sheet-flood and ephemeral-lake deposits. Although grain size characteristics and composition and diagenetic history are similar to overlying units of the Manitou Falls Formation, the Read Formation is characterized by a distinctive, overall low gamma-ray count (Mwenifumbo et al. 2007, Yeo et al., 2007) and is unconformably overlain by the Manitou Falls Formation (Long, 2007).

The Manitou Falls Formation is subdivided into three formal members: Bird (MFb), Collins (MFc) and Dunlop (MFd). The Bird member comprises interbedded sandstone and conglomerate. The Collins member consists of crossed-bedded, quartz arenite sandstone, minor pebbles and granules and conglomerate. The Dunlop member is recognized by its abundant intraclasts set in a medium to fine-grained quartz arenite sandstone. The clay-rich intraclasts are white to pale yellow, soft to silicified, generally 0.5–1.0 cm thick, and 3-5 cm long (Ramaekers et al., 2007; Yeo et al., 2007).

3. MATERIALS AND METHODS

Many drill holes were logged during the EXTECH IV project. For the Clay Mineral Studies Subproject 7, 18 drill holes were selected for detailed analyses (Table 1; Fig. 2). Based on the Stratigraphic and Sedimentology Subproject 4 (Ramaekers et al., 2007; Yeo et al., 2007) observations were made at every 1-m interval, and mostly recorded on a hand-held Palm III™ computer (Yeo et al., 2001). Key parameters of interest included maximum transported grain size in mm (MTG), percent grains greater than sand (% >2 mm), aggregate thickness and type of intraclasts, percent matrix clay, silicification and friability (Fig. 3).

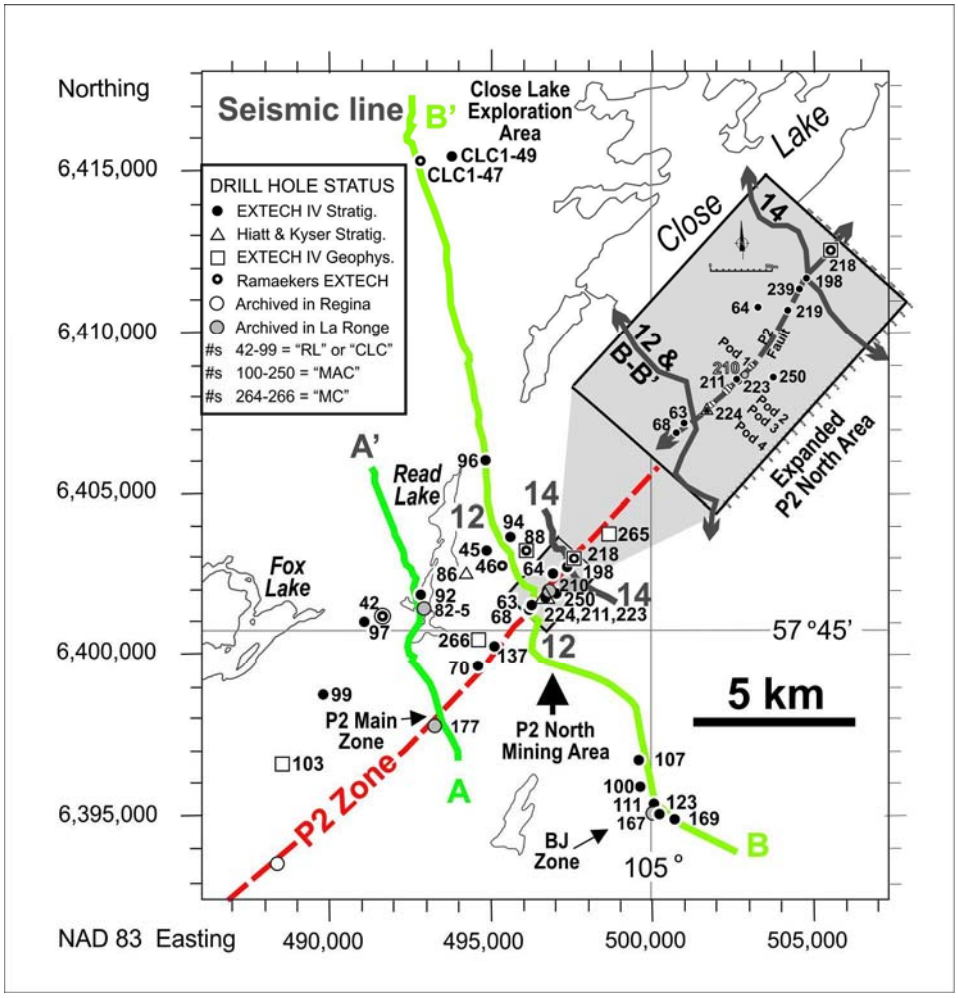

Figure 2: Location map of drill holes logged at the McArthur River uranium mine camp. Regional seismic reflection lines A-A' and B-B' are shown for context.

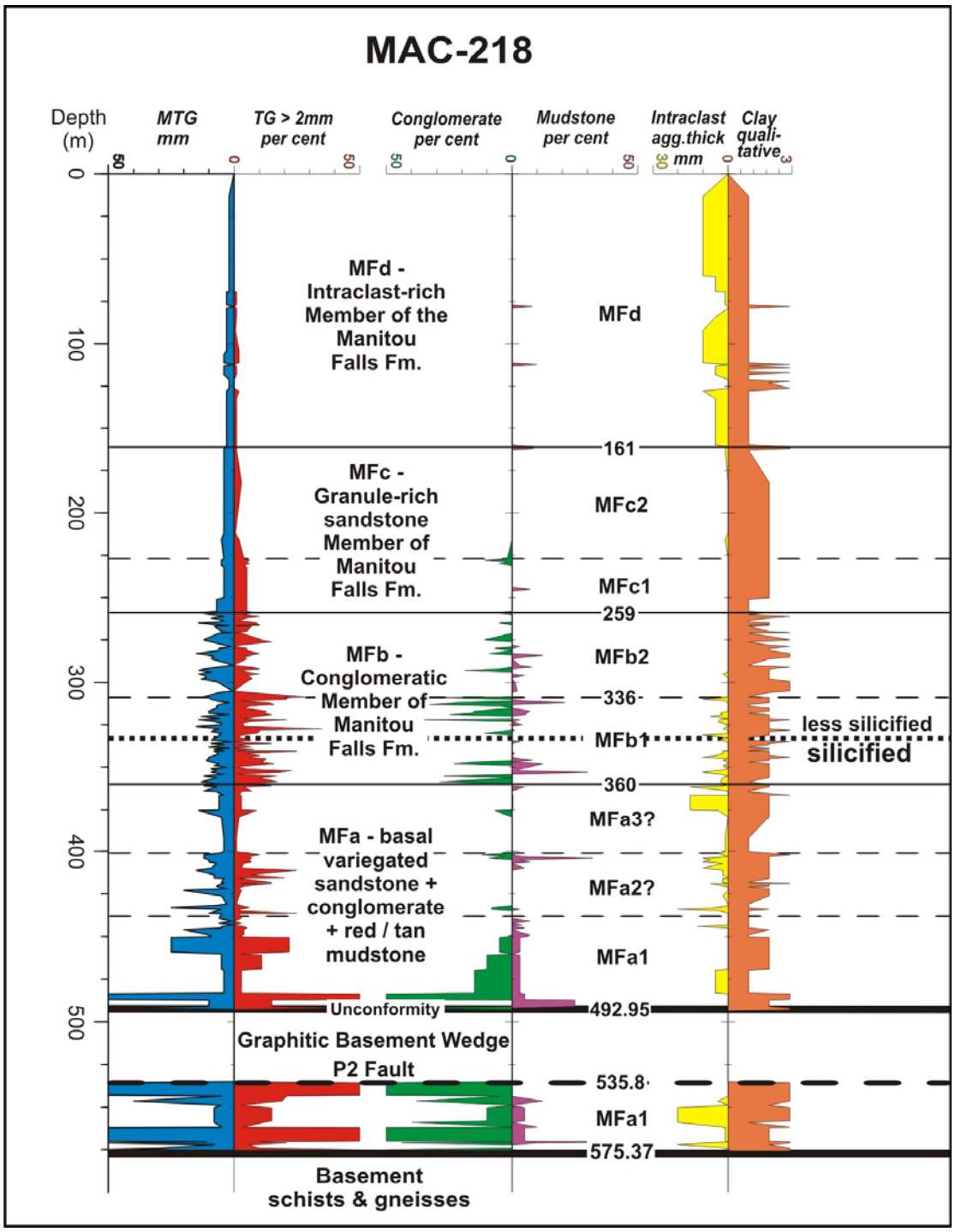

Figure 3: MAC-218 stratigraphic information based on core logging during the EXTECH IV program. Quantitative parameters include maximum transported grain (MTG) in mm; percent transported grains (TG) > 2 mm; percent conglomerate; percent mudstone, aggregate thickness of intraclasts in mm; and qualitative amount of clay in the matrix.

The samples selected for detailed mineralogical analyses included representative samples for the various lithological units, clay-rich interbeds, intraclasts and heavy mineral layers. The mineralogy of bulk powdered samples and clay-size separates was determined by X-ray powder diffraction (XRD) analysis. For clay-size separates, 40-mg suspensions (in distilled water) are pipetted onto glass slides and air-dried overnight to produce oriented mounts. X-ray patterns of the air-dried samples were recorded on a Philips PW1710 automated powder diffractometer equipped with a graphite monochromator, Co Kα radiation at 40 kV and 30 mA. The samples were also X-rayed following saturation with ethylene glycol and heat treatment (550 EC). Follow-up analyses were made using a Bruker D8 Advance equipped with a graphite monochromator, Co Kα radiation set at 40 kV and 40 mA. Semi-quantitative reduction of data was carried out using Jade (v.3.1) software (Materials Data, Inc.) as detailed in Percival et al. (2001).

Polished thin sections of layers containing interesting features and representative lithology were prepared at Vancouver Petrographics. All polished thins were impregnated with a blue dye to identify original porosity. Both petrographic and scanning electron microscopy were used to examine the polished thin sections in detail. In addition, grain mounts were made of various clay-rich samples for SEM and EDS analyses using a Leica Cambridge Stereoscan S360 SEM. The SEM was equipped with an Oxford/Link eXL-II energy-dispersion X-ray analyzer, Oxford/Link Pentafet Be window/light element detector, and an Oxford/Link Tetra backscattered electron detector. The SEM was operated at an accelerating voltage of 20kV. SEM images were captured at 768x576x256 greyscale and digitally stored for further processing.

All mineralogical hand specimens collected between 2000 and 2002 were analysed using a PIMA-II portable infrared spectrometer at Cameco Corporation's office in Saskatoon. The spectra were interpreted using the MINSPEC program (Earle et al., 1996). In 2002, MAC-198, MAC-218 and RL-064 were re-logged on a row-by-row basis and a representative sample was selected from each row for further analyses. These samples were split in the field, sun-dried and then analyzed *in situ* using both the PIMA-II and FieldSpec® Pro spectrometers for comparison.

Both the PIMA-II and FieldSpec® Pro (Analytical Spectral Devices, Inc.) instruments are field-portable infrared spectrometers that can provide rapid *in situ* qualitative to semi-quantitative clay mineral analyses. The PIMA-II instrument measures reflectance wavelengths from 1300 to 2500 nm (short-wavelength infrared region or SWIR) and mineral identification is based on the wavelength position and shape of absorption peaks. The FieldSpec® Pro measures reflectance wavelengths from 350 to 2500 nm that include the visible (350 - 780 nm), near infrared (780 - 1300 nm) and SWIR (1300 - 2500 nm) regions. Although the instruments operate with different detectors, other parameters are comparable. Spectral resolution for the PIMA-II is 7 nm for the SWIR region and for the FieldSpec® Pro resolution ranges from 3 nm in the visible and near infrared range, and up to 10 in the SWIR region. PIMA-II uses more spectral channels for the SWIR than the FieldSpec® Pro. As the FieldSpec® Pro was a relatively new acquisition at the time of sampling and analyses, the software to process the spectra in a similar manner to the PIMA-II spectra was not available. In order to provide some preliminary estimates of mineral content the spectra were processed in two stages. The spectra files were first converted from the FieldSpec® Pro format (350 to 2500 nm**)** to the PIMA format (1300 to 2500 nm) by extracting

just the SWIR wavelengths, and then processed using the MINSPEC program as noted above. For more information on the comparison of these instruments see Percival *et al.* (2002).

A few select samples containing alumino-phosphate (APS) minerals were examined using a transmission electron microscope (TEM) at CANMET for their identification (mineral group), composition and morphology. A Philips CM20 FEG TEM equipped with a Schottky field emission gun was operated at the voltage of 200 kV. The crystal structure of particles was determined using selected area electron diffraction (SAED) following conventional bright-field imaging. Chemical microanalysis used an Oxford Instrument thin-window energy-dispersive spectrometry (EDS) detector with an INCA system analyzer. A condenser aperture C2 of 50 mm and spot size 2 gave a beam diameter of 30 nm.

A 3 mm diameter sample (01JP27a) was cut using a Gatan ultrasonic disc cutter. The sample was embedded in Spurrs resin and cured. Ultramicrotomy was unsuccessful. The sample was then thinned by hand, grinding one side using diamond lapping film 30, 15, 9, 3, and 1 μm to attain a thickness of ~150 μm. A copper slotted grid was glued to the polished side for support. The other side was then thinned as above to a final thickness of about 100 μm. The sample was dimpled using a felt wheel and 0.25 μm diamond paste. The sample broke apart during dimpling and only a small piece of the reddish area was left (as viewed under a stereo microscope). The remaining sample was ion milled using a single beam modulation from the non-broken edge.

4. RESULTS

4.1 X-Ray Diffraction

Mineralogical results for the samples collected in the year 2000 are reported in Appendix A. Sample numbers or suites are organized by borehole as each is indicated by a unique PNA00 series, the GSC officer code for J.B. Percival. For most samples, only the clay-size (< 2 μm) fraction was analysed and reported, with the exception of MAC-218 where whole-rock mineralogy was also completed. The results are reported in wt% and reflect the composition of the clay-size fraction (or whole rock for MAC-218). Note that within the rock samples, the amount of clay-size material may only be about 3-5 wt% of the rock (i.e., matrix), however, many samples are clay-rich as they represent clay interbeds or intraclasts. Note that dickite is not differentiated from kaolinite by XRD and chlorite is commonly the sudoite variety.

4.1.1 Borehole MAC-100: Samples PNA00-01 to PNA00-64

In all, 87 samples and sub-samples of the clay-size fraction were analysed by XRD. The suite included sandstone, clay-rich interbeds and intraclasts. The sandstone samples contain abundant quartz, illite, chlorite and kaolinite and minor to trace amounts of tourmaline, hematite, siderite and goyazite. Chlorite and kaolinite dominate in the upper part of the borehole and illite increases with depth. Quartz ranges from non-detectable up to 60 wt%. Maximum concentrations for kaolinite, chlorite and illite are 90, 52 and 77 wt%, respectively. Tourmaline tends to be more abundant in the top half of the borehole (above 200 m) ranging from trace

amounts to 26 wt%. Hematite, siderite and goyazite were detectable in a few samples, mostly in trace amounts. Mixed-layer clay minerals (likely illite-smectite, I/S) are present in minor to trace amounts in most samples of the top half of the core, and in a few samples of the lower section.

The intraclasts (17 samples) are dominated by kaolinite, chlorite and/ or illite. Only a few samples contain quartz (up to 17 wt%) but two samples contain abundant tourmaline (56 to 73 wt%). The interbeds (12 samples) are dominated by kaolinite in the upper samples but illite in the lower samples. Quartz, chlorite and tourmaline range from trace amounts up to 70 wt%. Chlorite content increases at the expense of illite.

4.1.2 Borehole MAC-107: Samples PNA00-100 to PNA00-140

Forty-five sandstone, intraclast and interbed samples were selected from this borehole. In the clay-size fraction of the sandstone samples, quartz tends to dominate, but ranges from undetectable (one sample) to 70 wt% with a mean value of 33 wt%. Of the phyllosilicates, kaolinite dominates in the upper parts of the borehole and as it decreases, the illite content increases. Chlorite is variable throughout, but notably absent in some samples. Tourmaline is found in the upper parts of the borehole and in a few samples near the bottom (e.g., 330-370 m). Hematite is found in trace to minor amounts below 260 m depth. Goyazite and a mixed-layer clay mineral (I/S) occur in trace amounts throughout the borehole.

Four representative intraclast and 6 interbed samples were examined in detail. The intraclasts are dominated by kaolinite and chlorite, minor tourmaline and illite, and quartz is absent. The interbeds have similar compositions, with quartz being present in 2 of the 6 samples.

4.1.3 Borehole MAC-186: Samples PNA00-201 to PNA00-239

Eleven samples and sub-samples were selected from this borehole for detailed analyses, with a focus mainly on intraclasts. The clay-size fraction of the sandstone sample is dominated by illite (76 wt%) with minor quartz (17 wt%) and kaolinite (7 wt%). Of the 7 intraclast samples, 4 are dominated by kaolinite and the others by illite. Clay in the remaining interbed samples is illite.

4.1.4 Borehole MAC-189: Samples PNA00-301 to PNA00-337

All samples selected from this borehole are intraclasts composed of kaolinite and illite. Illite content increases with depth. Minor to trace amounts of chlorite, quartz, tourmaline, hematite, goethite, siderite, goyazite and anatase are also found. One sample contains 19 wt% quartz.

4.1.5 Borehole MAC-111: Samples PNA00-400 to PNA00-439

Two intraclast samples were analyzed by XRD. Both samples are dominated by tourmaline with minor kaolinite, illite chlorite and quartz.

4.1.6 Borehole RL-099: Samples PNA00-501 to PNA00-546

Five intraclast samples were selected; all are tourmaline-rich (54-89 wt%) with minor quartz, illite, chlorite, kaolinite and trace amounts of a mixed-layer clay minerals (I/S).

4.1.7 Borehole MAC-224: Samples PNA00-546B to PNA00-570

Three intraclast samples were analyzed and found to be similar to those in RL-099. They are dominated by tourmaline with minor kaolinite, illite, chlorite and quartz.

4.1.8 Borehole CLC10-77: Samples PNA00-601 to PNA00-630

The twelve samples examined are intraclasts selectively extracted from sandstone matrix. In contrast to the samples in RL-099 and MAC-224, these intraclasts are all dominated by kaolinite (59-94 wt%), except one. Illite is subordinate in the kaolinite samples and dominant in the twelfth sample. Quartz is measurable in the illite-rich intraclast. Chlorite and goyazite occur in trace amounts in some samples.

4.1.9 Borehole MAC-218: Samples PNA00-801 to PNA00-830

In this suite, 22 sandstone samples and 5 mudstone interbeds were analyzed for framework and clay-size mineralogy. The sandstone samples contain from 39 to 100 wt% quartz with a mean of 87 wt %. Most samples with less quartz contain kaolinite (undetectable up to 60 wt%) and minor to trace goethite. In the clay-size fraction, quartz dominates many of the samples, although kaolinite is present in almost all. A few samples contain minor illite and chlorite. One sample is dominated by tourmaline in the clay-size fraction. The five mudstone samples are similar in composition to the sandstone samples, for both the framework and clay-size fractions. Figure 4 shows the normalized abundances of matrix clay phases at 10 metre depth intervals down the drill hole based on XRD analyses.

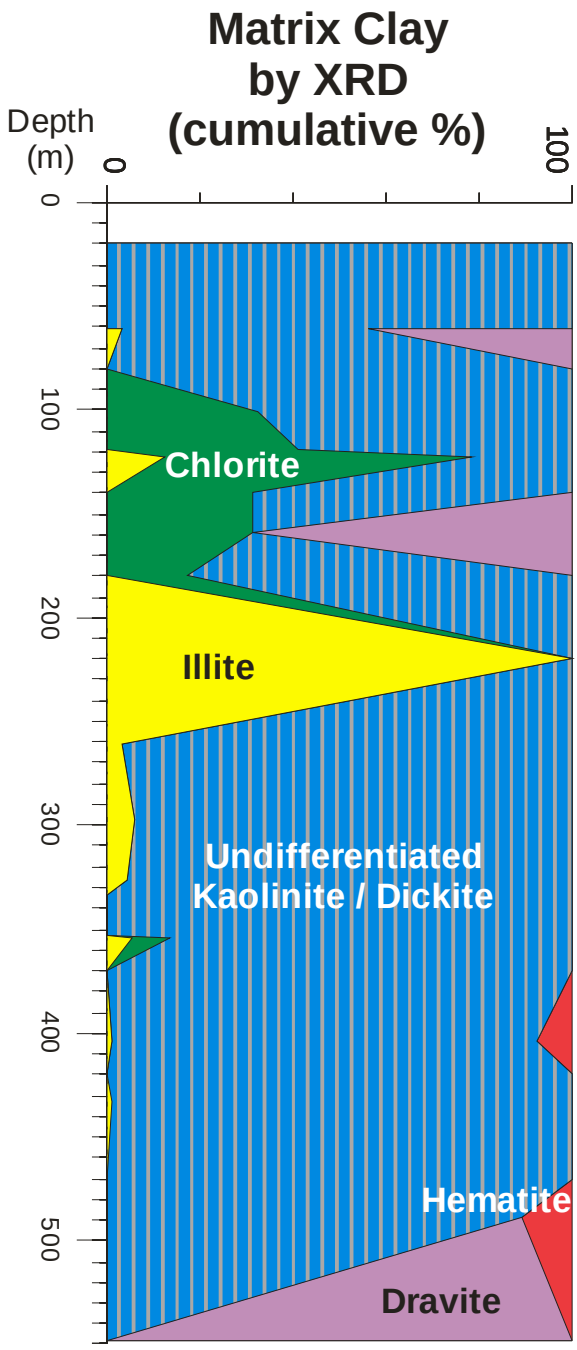

Figure 4. Illustration of mineralogical composition of the matrix in samples from MAC-218. Note the kaolin-group minerals (i.e., kaolinite and dickite) are undifferentiated by XRD.

Figure 5 illustrates textures and mineralogy of sandstone sample PNA00-822 at 352.72 m depth from MAC-218. The sample overall is a poorly sorted, interbedded mudstone and quartz arenite. The photomicrograph shows polycrystalline quartz grains, quartz overgrowths and a matrix of kaolin-group clay. Detailed SEM photomicrographs (Fig. 6) show textural relationships of detrital quartz and mica, and matrix clay. The kaolin-group mineral (in this case dickite based on results given below in infrared section) has a typical platy habit. Hematite coats mineral grains within pore spaces.

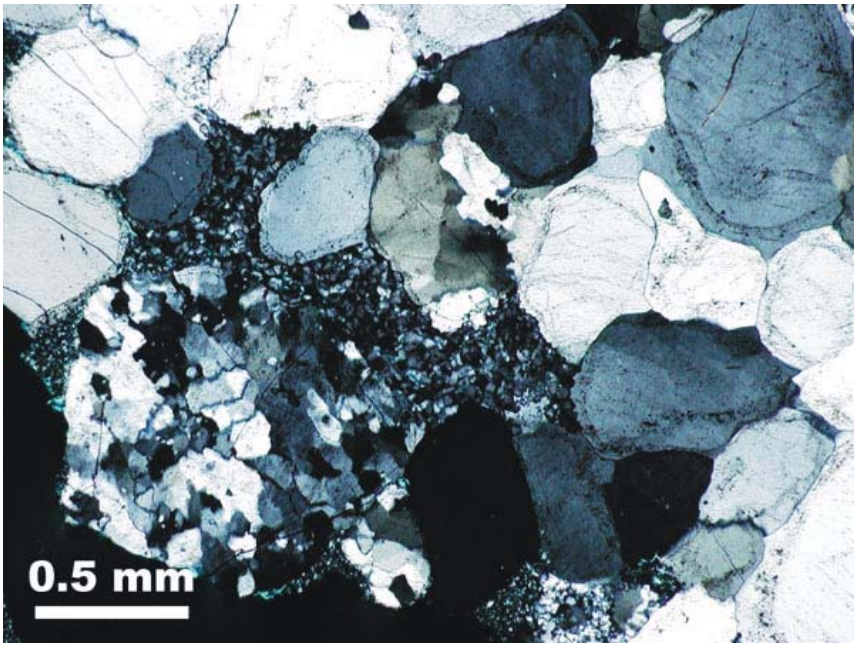

Figure 5: Sample PNA00-822 with polycrystalline quartz, quartz overgrowths and kaolin-group rich matrix (cross-polarized light, 5x objective).

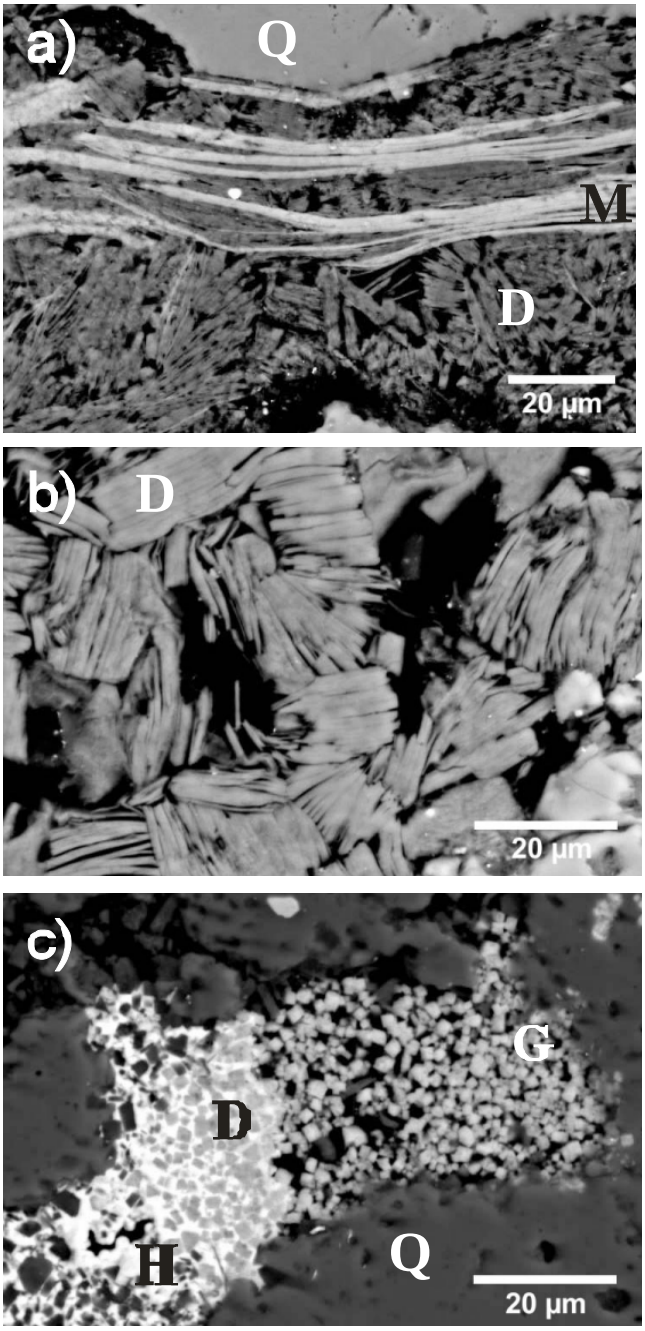

Figure 6. SEM photomicrographs of Sample PNA00-822 showing: a) detrital mica (M) in a dickite-rich (D) matrix; note alteration and feathering of layers; b) dickite displaying typical blocky texture; and c) hematite (H) forming a cement within intergranular pores and coating dickite (D); goyazite (G) has infilled the remaining part of the pore (BSI).

SEM photomicrographs of Sample PNA00-823 (354.2 m) are shown in Figure 7. Figure 7a is an overview of an intraclast-rich quartz arenite. Bright grains are zircon, and slightly less bright grains are rutile or anatase (Ti, O). Small intraclasts (IC) occur throughout the section. A close-up view of an intraclast (Fig. 7b) illustrates where illite (central) is surrounded by chlorite.

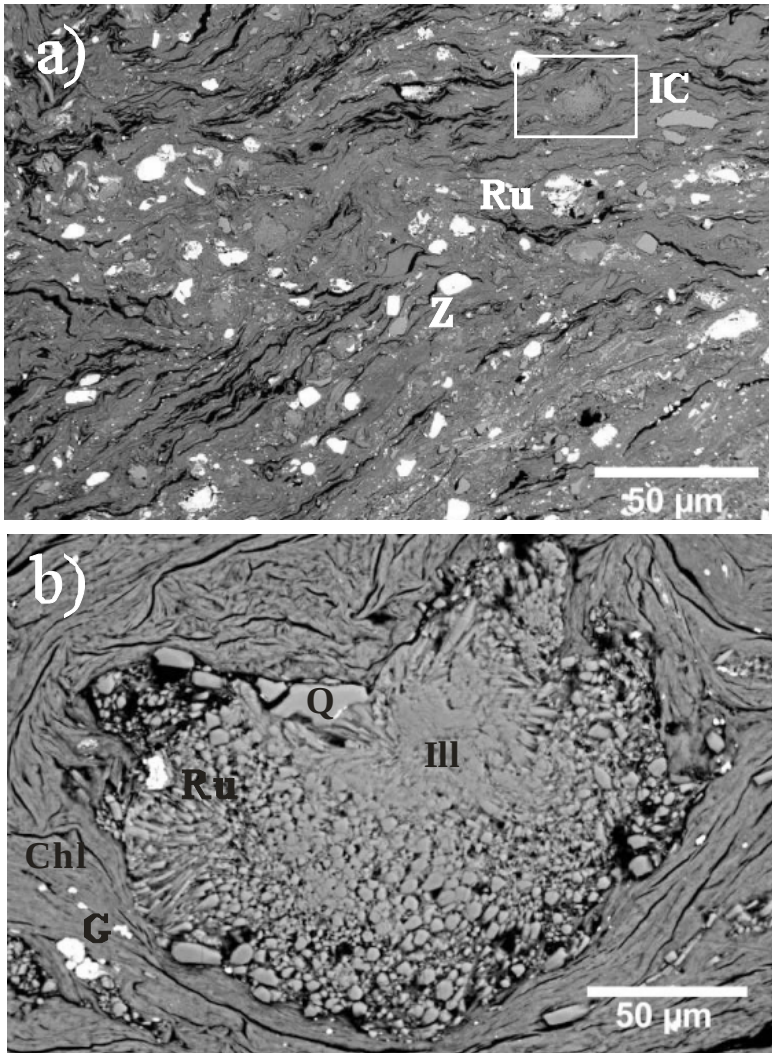

Figure 7: Sample PNA00-823 of a mudstone intraclast in a coarse-grained quartz arenite rich in heavy minerals, with a kaolinite and illite-rich matrix (IC=intraclast; RU=rutile; Z=zircon; Q=quartz; Ill=illite; Chl=chlorite; G=goyazite).

4.2 Infrared Spectroscopy-2000 Samples

Results of the PIMA-II/FieldSpec® Pro infrared analyses are summarized in Appendix B. The order of the boreholes is based on the sample numbers as each suite is indicated by a unique PNA00 series. Note that quartz is essentially infrared inactive using the PIMA-II instrument (SWIR wavelengths only). Thus, results are presented only for the following minerals: illite, chlorite, dickite, kaolinite, halloysite and dravite, hence all concentrations are reported in relative terms. No samples contain halloysite; chlorite is the tri-dioctahedral variety, sudoite. The higher the signal to noise ratio (reported in the last column), the better the quality of data. The lithofacies chosen for analyses were biased toward clay-rich zones, intraclasts and interbeds (mudstone). Comparison of results between the PIMA-II and FieldSpec® Pro instruments follows.

4.2.1 Borehole MAC-100: Samples PNA00-01 to PNA00-64

Clay-size minerals in this suite of samples are dominantly illite, kaolinite and chlorite. Dickite occurs in a few samples and tourmaline (dravite) is present in minor to trace amounts in all samples. Relative clay concentrations range from undetectable to 100, 63, and 80 wt% for illite, chlorite and kaolinite, respectively. Mean relative concentrations are 49, 13 and 25 wt% respectively. Dickite occurs in 18 samples below 190 m depth and chlorite tends to occur in the upper samples, above about 150 m.

4.2.2 Borehole MAC-107: Samples PNA00-100 to PNA00-140

Clay minerals in these samples are also dominated by illite and kaolinite. Mean relative concentrations are 47 and 33 wt%, respectively. Chlorite occurs in the central portion of the borehole and dickite occurs in a few samples. Tourmaline is found in samples from the upper part of the borehole (above 180 m) and generally in minor amounts (up to 33 wt%).

4.2.3 Borehole MAC-186: Samples PNA00-201 to PNA00-239

All clay-rich samples in this borehole are dominated by illite with a mean relative concentration of 69 wt%. A few samples contain kaolinite or dickite and chlorite was not detectable. Tourmaline occurs only in one sample, a pink to red sandstone.

4.2.4 Borehole MAC-189: Samples PNA00-301 to PNA00-337

The suite of clay-rich samples is composed of illite, kaolinite and/or dickite. Mean relative concentrations are 41, 22 and 33 wt%, respectively. Kaolinite dominates in some samples; in others it is subequal to dickite. Still other samples are dominated by dickite. No chlorite was detectable and tourmaline was detected in just two samples located near 200 m depth.

4.2.5 Borehole MAC-111: Samples PNA00-400 to PNA00-439

These samples contain illite, kaolinite, dickite and tourmaline with mean relative concentrations of 26, 34, 21 and 11 wt%, respectively. No chlorite was detectable. Illite varies with depth and in some samples where not present, kaolinite and tourmaline occur. As kaolinite declines with depth, dickite becomes more prominent, with a few exceptions. Tourmaline tends to occur in the upper parts of the borehole, above 150 m.

4.2.6 Borehole MAC-061: Samples PNA00-450 to PNA00-456

This small group of samples contains illite and kaolinite and no chlorite or tourmaline. Three samples contain dickite at the expense of kaolinite. Mean relative concentration for illite and kaolinite is 39 wt % each. No XRD analysis was attempted for these samples.

4.2.7 Borehole RL-099: Samples PNA00-501 to PNA00-546

The samples are chlorite-dominant with subordinate kaolinite, illite and tourmaline. No dickite was detected. Although the matrix clay appears to be chloritic, intraclasts are mostly illite-rich or kaolinite-rich with a few rich in tourmaline.

4.2.8 Borehole MAC-224: Samples PNA00-546B to PNA00-570

In contrast to samples from RL-099, these samples are dominated by kaolinite. Illite and tourmaline are abundant in some. Tourmaline tends to occur in the upper parts of the borehole and the lowermost samples. When tourmaline is low or absent, illite is more abundant. No chlorite was detected. Dickite is present in four samples in the lower part of the borehole (370-460 m).

4.2.9 Borehole CLC10-77: Samples PNA00-601 to PNA00-630

This group of samples contains abundant illite and dickite, with mean relative concentrations of 45 and 31 wt %, respectively. Kaolinite occurs in about a third of the samples examined. In a few samples, kaolinite and dickite co-exist in variable concentrations. Only one sample (603 m depth) contains chlorite and no samples contain tourmaline.

4.2.10 Borehole CLC10-76: Samples PNA00-631 to PNA00-632

Of the two samples analysed from this borehole one sample contains illite (45 wt%) and dickite (55 wt%); the other contains chlorite (59 wt%), illite (25 wt%) and kaolinite (15 wt%). The first sample is a bleached sandstone whereas the chlorite-bearing sample is a mudstone interbed.

4.2.11 Borehole MAC-218: Samples PNA00-801 to PNA00-830

This group is comprised mostly of illite and kaolinite. Chlorite and tourmaline dominate the samples above 200 m and dickite predominates in the lower section of the borehole, between about 330 and 470 m. Dickite and kaolinite tend to be mutually exclusive.

4.3 Infrared Spectroscopy-2001 Samples

These samples were collected in 2001 and the order of the boreholes is based on the sample numbers indicated by the PNA01 series. Other samples analyzed formed part of a M.Sc. thesis research by Sebastien Bernier (SBRL series; see Bernier, 2004). These data were collected in the field using a PIMA-II instrument (loaned by G. Drever, Cameco Corporation) on sandstone chips from boreholes RL-068, RL-063 and RL-046. The SBRL results are listed at the bottom of each worksheet in Appendix B.

4.3.1 Borehole RL-068: PNA01-001 to PNA01-054/SBRL-68 series

The samples analyzed in this drill hole tend to have mostly kaolinite and tourmaline. Illite is minor to moderate in most cases, although abundant in a few samples below 310 m. Chlorite occurs only in a few samples but dominates between 570 and 590 m. Dickite was found in only a few samples. These samples tend to comprise clay-rich material such as fracture fillings and intraclasts.

4.3.2 Borehole RL-63: PNA01-100/SBRL-63 series

Only one sample (two spots) was analyzed using the FieldSpec® Pro instrument (sample PNA01-100). Most samples examined by Bernier are from the bottom of the drill hole (~500-560 m). Illite and kaolinite dominate, chlorite occurs in one sample (553 m) and tourmaline is in a few samples.

4.3.3 Borehole RL-046: PNA01-200 to PNA01-209/SBRL-46 series

Only eleven samples were analyzed in this drill hole, including two by Bernier. All are illite-rich (25-100 wt%; mean=61.4 wt%) or kaolinite-rich (0-66 wt%; mean=32 wt%). Chlorite is present in one sample, dickite in 3 and tourmaline in 2.

4.3.4 Borehole CLC1-047: CL-47-01 to CL-47-37

Almost all samples are rich in illite and/or dickite. Illite ranges from ~8 - 100 wt% (mean = 52.7 wt%) and dickite from 0 to 92 wt% (mean = 42.2 wt%). Chlorite is present in only a few samples near the bottom of the drill hole. It dominates in one sample at 649 m (92.2 wt%) and is sub-equal to illite in another at 659 m. Kaolinite is present in one sample. Halloysite was suggested

by the algorithm in one sample but most likely the sample was still wet. Tourmaline was not found in any of the samples.

4.3.5 Borehole CLC1-049: CL-49-01 to CL-49-35

The samples in this drill hole have similar characteristics to those in CLC1-047. Almost all are illite- and/or dickite-rich. Exceptions are the few samples that contain chlorite (51-100 wt%) near the bottom of the hole (554, 564 and 584 m). Tourmaline was detected in only one sample at 574 m.

4.4 Infrared Spectroscopy-2002 Samples

The analyses for samples from these three boreholes (MAC-218-2, MAC-198 and RL-064) were made in 2002 on site. Both the Pima-II and the FieldSpec® Pro instruments were used in parallel on the exact same spots on each core. At least one representative sample was selected from each row of the core box. In addition, for these boreholes the presence of a kaolinite-dickite mixed layer mineral is reported (S_kaolinite) for several samples, based on changes made in the algorithm used to quantify the clay mineral species.

4.4.1 Borehole MAC-198: 02MAC198PA001to 02MAC198PA433 spectra files

The clay mineral content of samples from this drill hole is highly variable. Kaolinite and chlorite are abundant above 200 m and below 480 m. Dickite becomes prevalent between 200 and 500 m, and also occurs below 640 m. Note that 6 samples contain a dickite-kaolinite mixed-layer clay mineral (denoted S_kaolinite) ranging from 31 to 100 wt%, in association with just illite. Illite tends to occur in the middle to lower part of the borehole, but in some samples is completely absent. Minor tourmaline was found in about one-third of the samples at varying depths.

4.4.2 Borehole MAC 218-2: 02MAC218PA001 to 02MAC218PA333 spectra files

The upper part of this borehole above ~ 210 m and the lower part below 490 m are dominated by chlorite and kaolinite. Dickite becomes prevalent and increasingly abundant between 230 and 490 m. Illite is rare in the upper section (< 198 m) and increases in abundance with depth. However, illite may be absent in some samples in the lowermost section. Tourmaline occurs in the zones along with chlorite and kaolinite in slightly abundant to minor amounts, ranging from about 6 - 27 wt%. Three samples were found to contain a dickite-kaolinite mixed-layer clay mineral

4.4.3 Borehole RL-64: 02RL064PA001 to 02RL064PA379 spectra files

Clay minerals in this suite of samples appear similar in composition to those of MAC-198 and MAC-218. Samples tend to contain kaolinite and chlorite in the upper part of the borehole (< 250 m). In this zone, dickite is absent, illite is absent to minor and tourmaline occurs in minor amounts. Below this depth, kaolinite decreases and was detected in only a few small zones,

whereas illite content increases. Dickite is in greater proportion below 300 m and tourmaline essentially disappears except in a few samples. Note that as in MAC-198, there are 4 samples that contain a kaolinite-dickite mixed-layer mineral, in association with illite.

4.5 Comparison of PIMA and FieldSpec® Pro Analyses

As reported above, several boreholes (MAC-198, MAC-218 and RL-64) were analysed using both a PIMA-II and FieldSpec® Pro instruments in 2002. The spectra from both instruments were processed using the same algorithm after converting the fuller FieldSpec® Pro spectrum (VIS, NIR and SWIR) into a PIMA-like spectrum (i.e., from 1350 to 2500 nm). Overall results from this study were discussed by Percival et al. (2002). For a brief comparison of the two sets of results, their plots are reproduced here as Figures 8 to 10. Note that these analyses do not represent the overall bulk mineralogy but specifically targeted the relative abundance of the clay minerals observed in matrix, interbeds and intraclasts.

Figure 8 shows that the matrix mineralogy for samples from borehole MAC-198 was almost identically detected by the two instruments. Clays in the upper section (< 200 m) are dominated by kaolinite with variable amounts of chlorite (variety sudoite) and tourmaline (dravite). Minor to trace amounts of illite occur in most samples across the entire depth of the borehole. Between 200 and 400 m, illite dominates and then decreases with depth as dickite content increases from 300 to 480 m. Below the unconformity (485 m), basement rocks contain abundant chlorite. Dickite may include a kaolinite-dickite mixed-layer clay mineral.

Borehole MAC-218 (Figure 9) shows a similar mineralogical distribution with depth. The upper section (< 200 m) is dominated by kaolinite, chlorite, minor dravite and variable amounts of illite. At about 200 m the mineralogy changes sharply. Below this, illite dominates but decreases with depth as dickite content increases. There is another sharp change at around 490 m (near the unconformity); the basement rocks are chlorite-rich.

Borehole RL-064 (Figure 10) contains abundant kaolinite above 200 m and variable amounts of chlorite. Dravite content increases between 100 and 260 m and the higher proportions occur in an intraclast-rich zone. The change from kaolinite-dominant to illite occurs at the base of the MFc, at ~260 m. From this point until the unconformity (~ 531 m) dickite is abundant in distinct zones. The few basement rocks analysed contain abundant illite and only traces of chlorite.

Standards were used to validate the results from both instruments. Percival et al. (2002) reported that although the mineralogy is highly comparable, illite content seemed to be enhanced using the FieldSpec® Pro and tourmaline (dravite) by the Pima-II instrument. Confirmation was made using XRD analyses. For example, Figure 11 shows the PIMA-II analyses of the matrix mineralogy for the same suite of samples analysed by XRD (see Figure 4) normalizing the clay mineral data without quartz. Note that kaolinite shown in Figure 4 is undifferentiated using XRD analyses and PIMA-II does not see oxide minerals such as hematite that are detectable by the FieldSpec® Pro in the VIS region. Thus a direct comparison is not entirely possible. For future studies, a similar algorithm is required to process the FieldSpec® Pro data to determine

modal mineralogy. In addition, within this algorithm it will be critical to quantify the abundance of quartz in these types of samples.

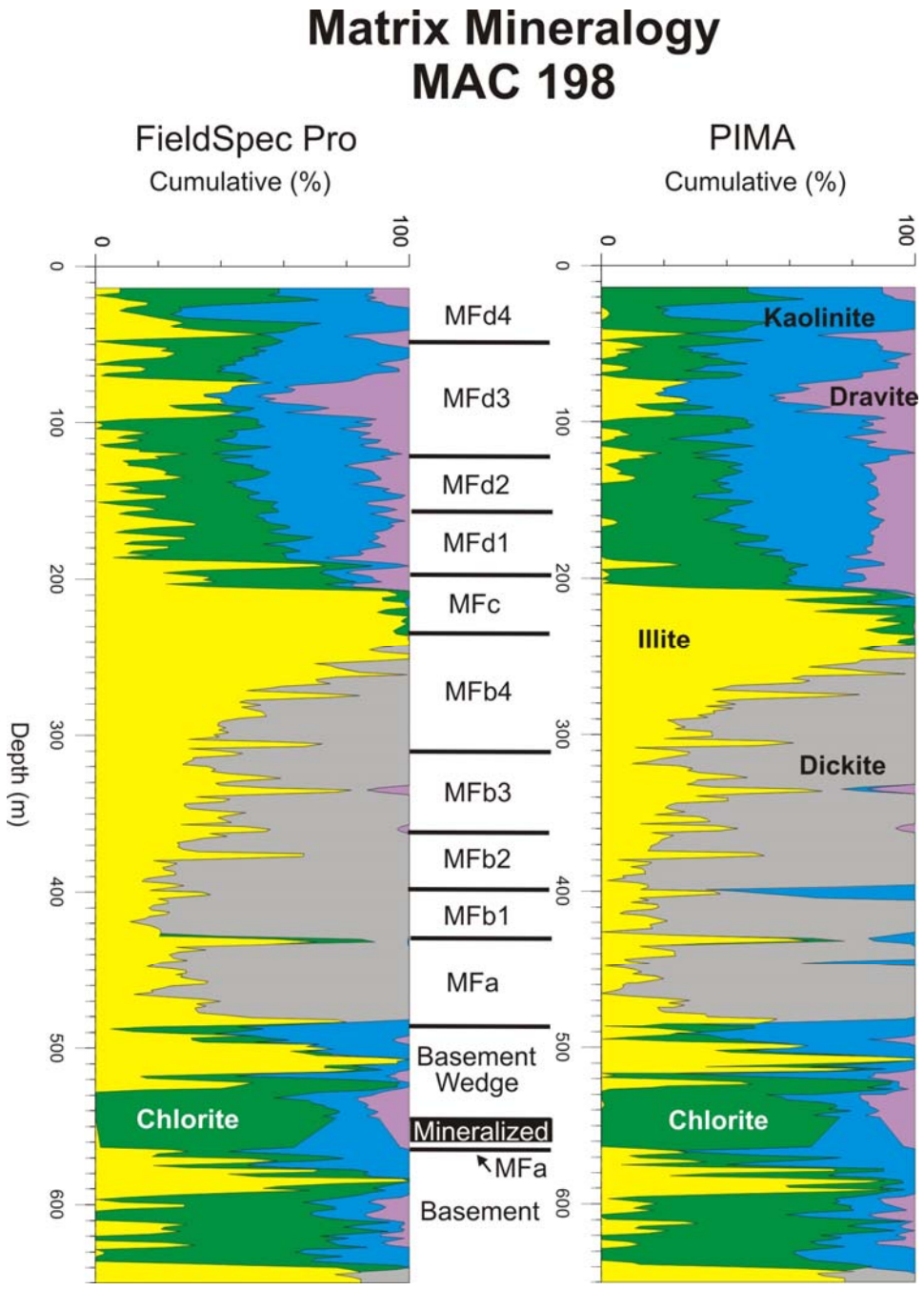

Figure 8: Matrix mineralogy as determined by FieldSpec® Pro and PIMA-II instruments for MAC-198 samples.

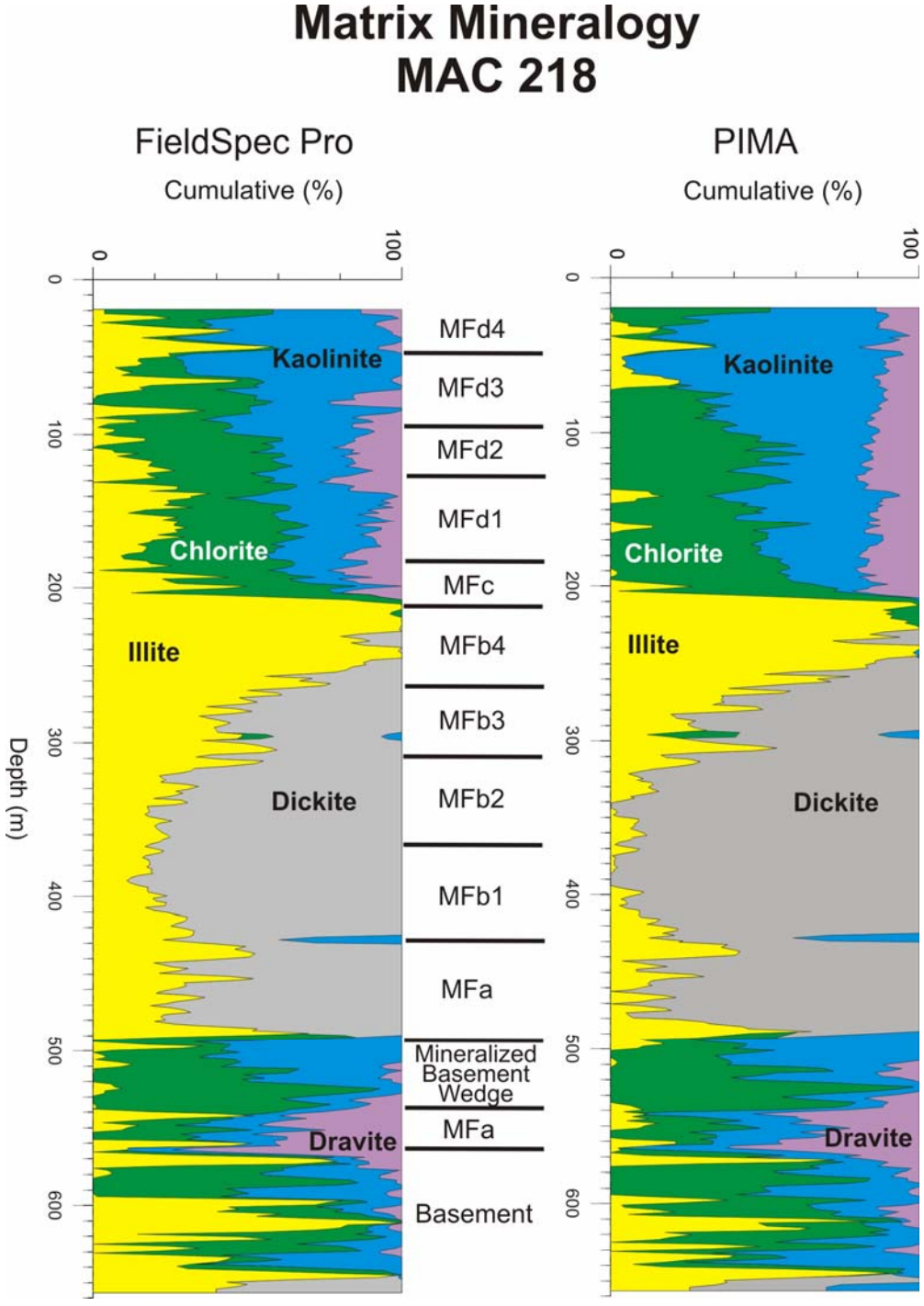

Figure 9: Matrix mineralogy as determined by FieldSpec® Pro and PIMA-II instruments for MAC-218 samples.

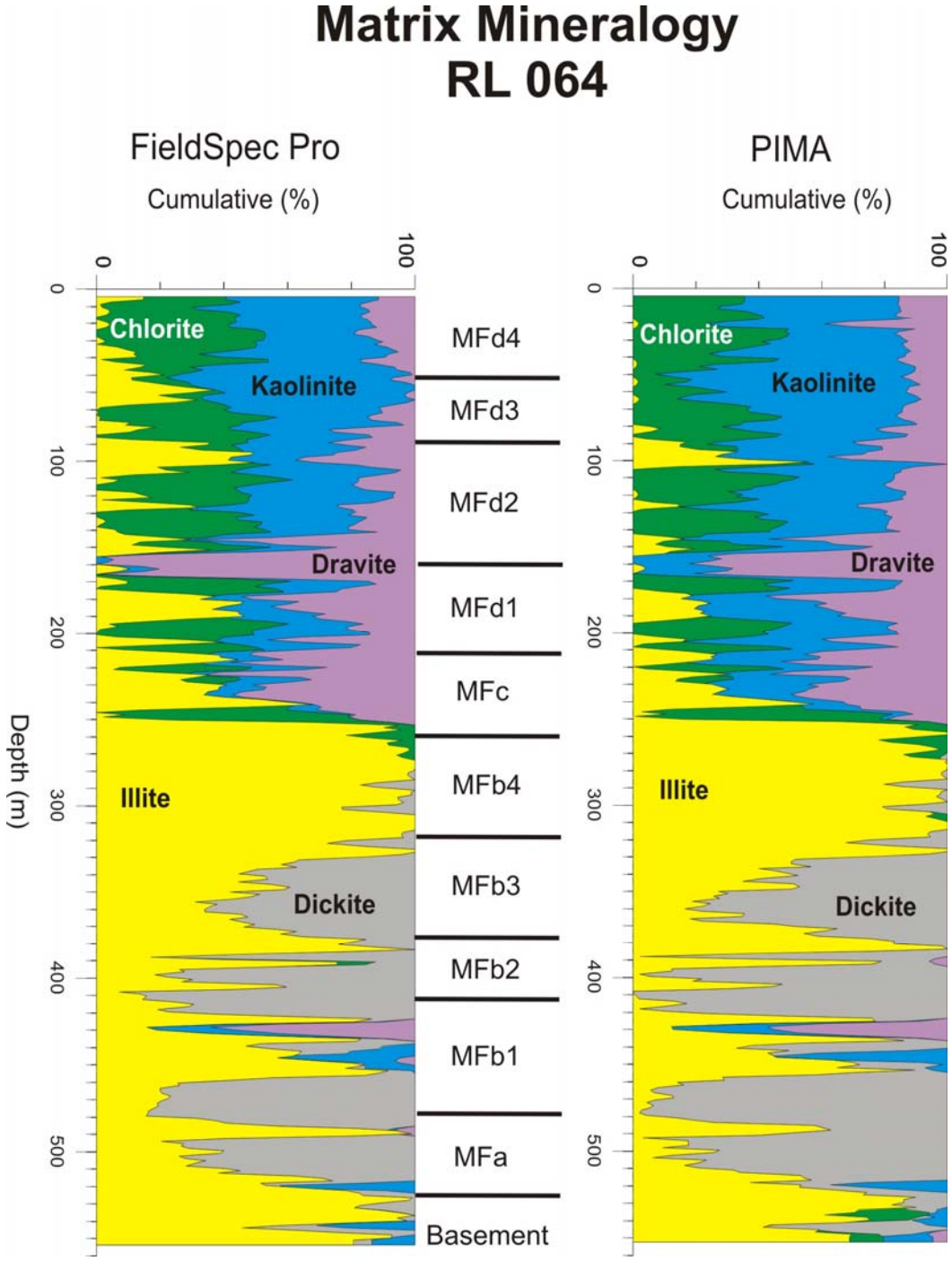

Figure 10: Matrix mineralogy as determined by FieldSpec® Pro and PIMA-II instruments for RL-064 samples.

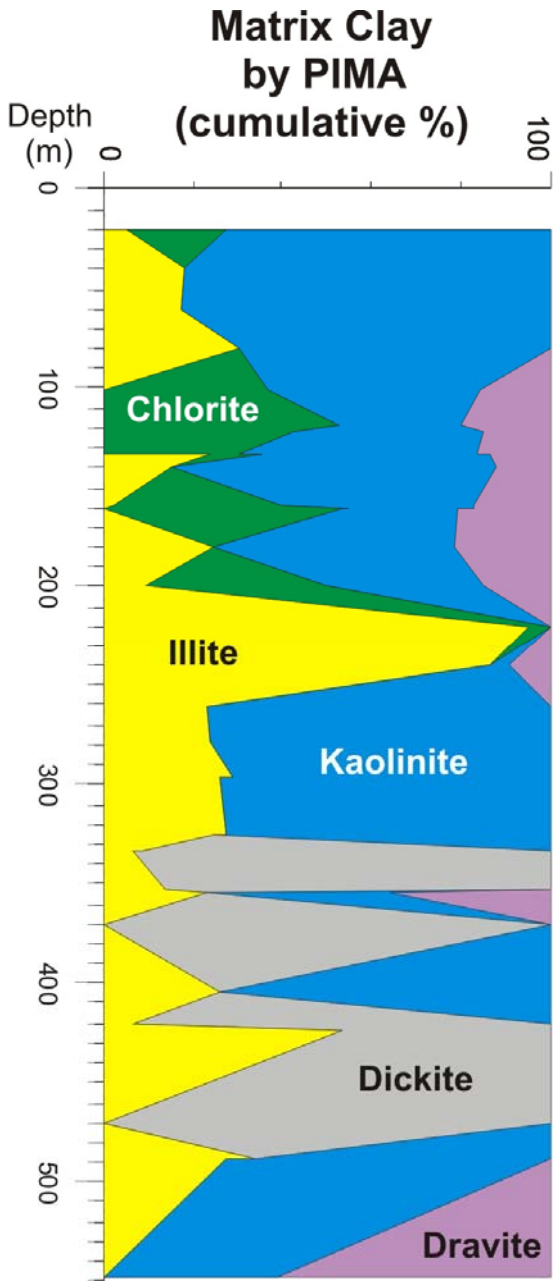

Figure 11: Mineralogical composition of the matrix clay in selected samples from MAC-218 based on PIMA-II analyses (direct comparison to Figure 4).

4.6 TEM Study of APS Minerals

In the course of study during the EXTECH IV program, many samples were examined under the SEM. There was special interest in the APS minerals as they may relate to genesis of the uranium deposits with respect to peak diagenesis and/or hydrothermal alteration. Wilson (1985) first described the crandallite-group minerals occurring in all units of the Athabasca Group in the western part of the Athabasca Basin. He suggested these were authigenic or early diagenetic in origin. Percival (1989) observed similar minerals associated with illite within the bleached zones surrounding the Cigar Lake uranium deposit and determined these to be goyazite or florencite (REE-bearing). Mwenifumbo and Bernius (2007) reported that the thorium content in conglomeratic layers in the McArthur river area, as detected by spectral gamma-ray logs, was highly correlated to thorium-bearing APS minerals. Based on their detailed analyses, the APS minerals appear to be goyazite ($SrAl_3(PO_4)_2(OH)_5AH_2O$) with thorium-rich centres (Fig. 12). The TEM work reported here is a follow-up to their study, attempting to determine the origin of these minerals. The question asked was whether the thorium-rich cores could have originated from detrital minerals such as monazite or diagenetic minerals such as xenotime.

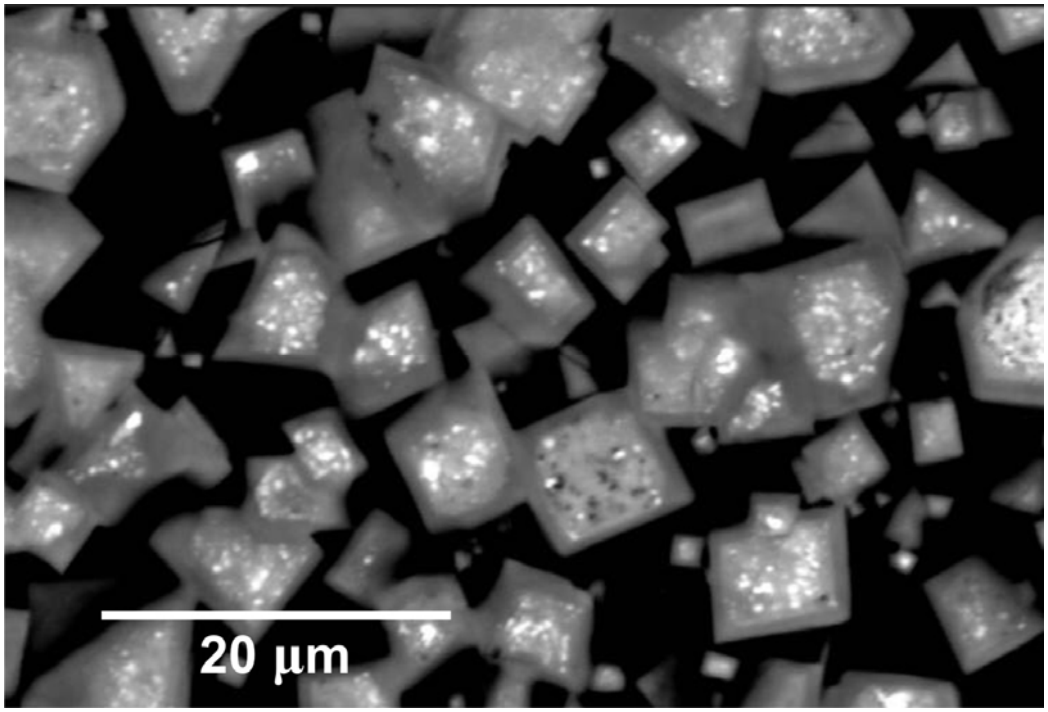

Figure 12: Crandallite-group minerals (goyazite) with Th-rich (bright areas) centres (Sample 01JP27a).

The crandallite group (or plumbogummite group; Mandarino and Back, 2004) has the general formula: $AB_3(XO_4)_2(OH,F)_5$ or $AB_3(XO_4)_2(OH,F)_6$ where A=Ba, Bi, Ca, Ce, La, Nd, Pb, Sr, Th; and B=Al, Fe^{+3}; As, P, Si; and X=As, P, Si (Mandarino, 1999). In most samples observed under the SEM, the mineral goyazite (Sr variety) was the most common. Some, as illustrated above (Fig. 12), contain thorium-rich centres, others contain cerium or other REEs suggesting they are the florencite variety.

A small APS-rich area was drilled from the thin section of sample 01JP27a to obtain a suitable specimen for TEM analyses. Selected area electron diffraction (SAED) (Figure 13-see end of report) was completed on several spots. According to V. Guertsman (Personal Communication, 2004) the patterns could match goyazite or crandallite structure (trigonal *R3m* with very close lattice parameters – a = 0.70 nm and c = 1.65 nm), possibly match brabantite (monazite-group, monoclinic structure) and less likely to the thorianite structure. The EDS chemistry (Table 2) supports the goyazite (or crandallite) mineral, less so for brabantite or thorianite. Thus, the TEM work appears to be somewhat inconclusive as to what the precursor mineral may have been to form the thorium-bearing goyazite. The origin of the thorium may have been monazite as only one monazite grain was observed in the samples studied by Mwenifumbo and Bernius (2007) whereas monazite should have been a common detrital heavy mineral. It is possible that thorium released by alteration of monazite replaced Ca or Sr in the crandallite-group minerals as they formed rather than the APS minerals growing around a monazite core. Just such a reaction was reported by Madore et al. (2000) in basement leucogranitic rocks. Further analyses are required to determine the composition of the cores of these minute crystals.

5. SUMMARY

This report collates and compares mineralogical analyses of clay-sized minerals obtained from many drill holes in the McArthur River area of the Athabasca Basin, Saskatchewan. Both portable (field) infrared analyses and (laboratory) X-ray diffraction (XRD) analyses were obtained on many duplicate samples as a test of different analytical methods to determine mineralogy and to provide legacy baseline data. About 300 samples from 9 boreholes were analysed using XRD. These analyses are semi-quantitative (wt%) and targeted selected samples. About 1900 spot analyses from samples from 18 boreholes were acquired using PIMA-II and/or FieldSpec® Pro infrared spectrometers. The suite of samples analysed by both these instruments is relatively complete down several boreholes from the McArthur River uranium mine camp. In addition, a brief comparison of the results of both infrared instruments is provided. Discussion of results from a follow-up study using the TEM to analyse alumino-phosphate minerals (APS) is included for completion.

6. ACKNOWLEDGEMENTS

This work was supported by the EXTECH IV — Athabasca Uranium Multidisciplinary Study. Drill core access was generously provided by AREVA Resources Canada Inc. and Cameco Corporation along strategic targets. Use of the PIMA-II instrument and interpretation of data was

provided by Cameco Corporation. The authors are grateful to the following students for their assistance in the field and great discussions: C. Williamson, S. Bosman, S. Russell, S. Bernier, B. Collier, A. Gaze, and A. Grimeau. Laboratory work was assisted by several students (co-authors) and secondary school co-op students P. Puetz and M.-A. Hartlin. We are also grateful to K. Nguyen (GSC) for cartographic assistance. Special thanks to V. Guertsman (CANMET) for his insights on interpreting the SAED patterns of the APS minerals. We thank C.W. Jefferson for critical review of this report and with G. Delaney (Saskatchewan Geological Survey) for their leadership throughout this EXTECH IV project.

7. REFERENCES

Bernier, S.2004. Stratigraphy of the Late Paleoproterozoic Manitou Falls Formation, in the vicinity of the McArthur River uranium deposit, Athabasca Basin, Saskatchewan, Canada; M.Sc. Thesis, Laurentian University, Sudbury, Ontario, 184 p.

Earle, S., Wheatley, K. and Wasyliuk, K. 1996. Application of reflectance spectroscopy to the assessment of alteration mineralogy in the Key Lake area; in Proceedings of Minexpo '96 Symposium, (eds.) K.E. Ashton and C.T. Harper; Advances in Saskatchewan Geology and Mineral Exploration, Special Publication 14, p.109-123.

Hiatt, E.E. and Kyser, T.K. 2007. Sequence stratigraphy, hydrostratigraphy, and mineralizing fluid flow in the Proterozoic Manitou Falls Formation, eastern Athabasca Basin, Saskatchewan; in EXTECH IV: Geology and Uranium Exploration TECHnology of the Proterozoic Athabasca Basin, Saskatchewan and Alberta, (eds.) C.W. Jefferson and G. Delaney; Geological Survey of Canada, Bulletin 588 (also Saskatchewan Geological Society, Special Publication 18; Geological Association of Canada, Mineral Deposits Division, Special Publication 4), p. 489-506.

Hoeve, J. and Quirt, D. 1984. Mineralization and host rock alteration in relation to clay mineral diagenesis and evolution of the Middle-Proterozoic, Athabasca basin, northern Saskatchewan, Canada; Saskatchewan Research Council, Technical Report 187, 187 p.

Jefferson, C.W. and Delaney, G. 2001. Multidisciplinary EXTECH IV Athabasca uranium study: Project update; in Summary of Investigations 2001, v. 2, Saskatchewan Geological Survey, Saskatchewan Energy and Mines, Miscellaneous Report 2001-4.2, p. 187-198.

Jefferson, C.W. and Delaney, G. (eds.). 2007. EXTECH IV: Geology and Uranium EXploration TECHnology of the Proterozoic Athabasca Basin, Saskatchewan and Alberta; Geological Survey of Canada, Bulletin 588 (*also* Saskatchewan Geological Society, Special Publication 18; Geological Association of Canada, Mineral Deposits Division, Special Publication 4), 644 p.

Jefferson, C.W., Percival, J.B., Bernier, S., Cutts, C., Drever, G., Jiricka, D., Long, D., McHardy, S., Quirt, D., Ramaekers, P., Wasyliuk, K. and Yeo, G.M. 2001. Lithostratigraphy and mineralogy in the eastern Athabasca Basin, northern Saskatchewan - Progress in year 2 of

EXTECH IV; in Summary of Investigations 2001, v. 2, Saskatchewan Geological Survey, Sask. Energy Mines, Misc. Rept. 2001-4-2, p. 272-290.

Keller, W.D. 1970. Environmental aspects of clay minerals; Journal Sedimentary Petrology, 40, p. 788-813.

Kisch, H.J. 1983. Mineralogy and petrology of burial diagenesis (burial metamorphism) and incipient metamorphism in clastic rocks; in Diagenesis in Sediments and Sedimentary Rocks, (eds.) G. Larsen, G. and G.V. Chilingar; v. 2, Elsevier, Amsterdam, p. 289-493.

Long, D.G.F. 2007. Topographic influences on the sedimentology of the Read and Manitou Falls formations, eastern Athabasca Basin, Saskatchewan; in EXTECH IV: Geology and Uranium Exploration TECHnology of the Proterozoic Athabasca Basin, Saskatchewan and Alberta, (eds.) C.W. Jefferson and G. Delaney; Geological Survey of Canada, Bulletin 588 (also Saskatchewan Geological Society, Special Publication 18; Geological Association of Canada, Mineral Deposits Division, Special Publication 4), p. 267-280.

Madore, C., Annesley, I. and Wheatley, K. 2000. Petrogenesis, age, and uranium fertility of peraluminous leucogranites and pegmatites of the McClean Lake/Sue and Key Lake/P-Patch deposit areas, Saskatchewan; GeoCanada: The Millennium Geoscience Summit. Joint Meeting of the Canadian Geophysical Union, Canadian Society of Exploration Geophysicists, Canadian Society of Petroleum Geologists, Canadian Well Logging Society, Geological Association of Canada, and the Mineralogical Association of Canada. May 29-June 2, Calgary, Alberta (also GAC-MAC Program With Abstracts v. 25), 1041.pdf, 4 p (extended abstract).

Mandarino, J.A. 1999. Fleisher's Glossary of Mineral Species. 8th Edition. The Mineralogical Record Inc., Tucson, Arizona.

Mandarino, J.A. and Back, M.E. 2004. Fleisher's Glossary of Mineral Species. 9th Edition. The Mineralogical Record Inc., Tucson, Arizona

Mwenifumbo, C.J. and Bernius, G.R 2007. Crandallite-group minerals: host of thorium enrichment in the eastern Athabasca Basin, Saskatchewan; in EXTECH IV: Geology and Uranium Exploration TECHnology of the Proterozoic Athabasca Basin, Saskatchewan and Alberta, (eds.) C.W. Jefferson and G. Delaney; Geological Survey of Canada, Bulletin 588 (also Saskatchewan Geological Society, Special Publication 18; Geological Association of Canada, Mineral Deposits Division, Special Publication 4), p. 521-532.

.

Mwenifumbo, C.J., Percival, J.B., Bernius, G.R., Elliott, B., Jefferson, C.W., Wasyliuk, K. and Drever, G. 2007. Comparison of geophysical, mineralogical, and stratigraphic attributes in drillholes MAC-218 and RL-88, McArthur River uranium camp, Athabasca Basin, Saskatchewan; in EXTECH IV: Geology and Uranium Exploration TECHnology of the Proterozoic Athabasca Basin, Saskatchewan and Alberta, (eds.) C.W. Jefferson and G. Delaney; Geological Survey of Canada, Bulletin 588 (also Saskatchewan Geological Society,

Special Publication 18; Geological Association of Canada, Mineral Deposits Division, Special Publication 4), p. 507-520.

Percival, J.B.M. 1989. Clay mineralogy, geochemistry, and partitioning of uranium within the alteration halo of the Cigar Lake uranium deposit, Saskatchewan, Canada; Ph.D. Thesis, Carleton University, Ottawa, Ontario, 592 p.

Percival, J.B., Bell, K. and Torrance, J.K. 1993. Clay mineralogy and isotope geochemistry of alteration associated with the Cigar Lake deposit; Canadian Journal Earth Sciences, 30, p. 689-704.

Percival, J.B., Bosman, S.A., Venance, K.E., Hunt, P.A., Ramaekers, P. and Jefferson, C.W. 2009. Origin of enigmatic beds in Proterozoic sandstone, Athabasca basin, Saskatchewan, Canada. 14th International Clay Conference, Italy (June 2009), Book of Abstracts, v. 1-Oral Sessions, p. 192

Percival, J.B., Hunt, P. and Wygergangs, M. 2001. Mineralogical investigations of Canadian till and lake- and stream-sediment reference materials: Part 1. Standardized X-ray diffraction and scanning electron microscope methods; Geological Survey of Canada, Current Research 2001-E9, 8 p.

Percival, J.B., Wasyliuk, K., Reif, T., Bernier, S., Drever, G., and Perkins, C.T. 2002. Mineralogical aspects of three drill cores along the McArthur River transect using a portable infrared spectrometer; in Summary of Investigations 2002, v. 2, Saskatchewan Geological Survey, Saskatchewan Industry and Resources, Miscellaneous Report. 2002-4.1.

Ramaekers, P. 1979. Stratigraphy of the Athabasca basin; in Summary of Investigations 1979; Saskatchewan Geological Survey, Miscellaneous Report 79-10, p. 154-160.

Ramaekers, P. 1980. Stratigraphy and tectonic history of the Athabasca Group (Helikian) of northern Saskatchewan; in Summary of Investigations 1980; Saskatchewan Geological Survey, Miscellaneous Report 80-4, p. 99-106.

Ramaekers, P. 1981. Hudsonian and Helikian basins of the Athabasca region, northern Saskatchewan; in Proterozoic Basins of Canada, (ed.) F.H.A. Campbell; Geological Survey of Canada, Paper 81-10, p. 219-233.

Ramaekers, P. 1983. Geology of the Athabasca Group, NEA/IAEA Athabasca basin test area; in Uranium Exploration in Athabasca Basin, Saskatchewan, Canada, (ed.) E.M. Cameron; Geological Survey of Canada, Paper 82-11, p. 15-25.

Ramaekers, P. 1990. Geology of the Athabasca Group (Helikian) in northern Saskatchewan; Saskatchewan Energy and Mines, Saskatchewan Geological Survey, Report 195, 49 p.

Ramaekers, P., Jefferson, C.W., Yeo, G.M., Collier, B., Long, D.G.F., Drever, G. McHardy, S., Jiricka, D., Cutts, C., Wheatley, K., Catuneanu, O., Bernier, S., Kupsch, B. and Post, R.T.

2007. Revised geological map and stratigraphy of the Athabasca Group, Saskatchewan and Alberta; in EXTECH IV: Geology and Uranium Exploration TECHnology of the Proterozoic Athabasca Basin, Saskatchewan and Alberta, (eds.) C.W. Jefferson and G. Delaney; Geological Survey of Canada, Bulletin 588 (also Saskatchewan Geological Society, Special Publication 18; Geological Association of Canada, Mineral Deposits Division, Special Publication 4), p. 155-191.

Sibbald, T.I.I. 1985. Geology and genesis of the Athabasca basin uranium deposits; in Summary of Investigations 1985. Saskatchewan Geological Survey, Miscellaneous Report 85-4, p. 133-156.

Wilson, J.A. 1985. Crandallite group minerals in the Helikian Athabasca Group in Alberta, Canada; Canadian Journal of Earth Sciences, 22, p. 637-641.

Yeo, G. and Delaney, G. 2007. The Wollaston Supergroup, stratigraphy and metallogeny of a Paleoproterozoic Wilson cycle in the Trans-Hudson Orogen, Saskatchewan; in EXTECH IV: Geology and Uranium Exploration TECHnology of the Proterozoic Athabasca Basin, Saskatchewan and Alberta, (eds.) C.W. Jefferson and G. Delaney; Geological Survey of Canada, Bulletin 588 (also Saskatchewan Geological Society, Special Publication 18; Geological Association of Canada, Mineral Deposits Division, Special Publication 4), p.89-117.

Yeo, G., Jefferson, C., Ramaekers, P. and Tong, K. 2001. From palm to plot: Core logging in the EXTECH IV Athabasca Basin stratigraphy sub-project; in Summary of Investigations 2001, v.2, Saskatchewan Geological Survey, Saskatchewan Energy and Mines, Miscellaneous Report 2001-4-2, p. 314-320.

Yeo, G.M., Jefferson, C.W. and Ramaekers, P**.** 2007. Comparison of lower Athabasca Group stratigraphy among depositional systems, Saskatchewan and Alberta; in EXTECH IV: Geology and Uranium Exploration TECHnology of the Proterozoic Athabasca Basin, Saskatchewan and Alberta, (eds.) C.W. Jefferson and G. Delaney; Geological Survey of Canada, Bulletin 588 (also Saskatchewan Geological Society, Special Publication 18; Geological Association of Canada, Mineral Deposits Division, Special Publication 4), p. 465-488.

Figure 13: Selected area electron diffraction (SAED) patterns of sample 01JP27a in left hand column for several spots compared to goyazite, brabantite (monazite-group) and thorianite.

DP #	Matching interplanar spacings →	Goyazite	Brabantite	Thorianite
S620	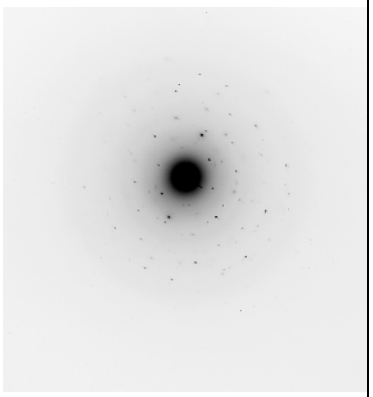	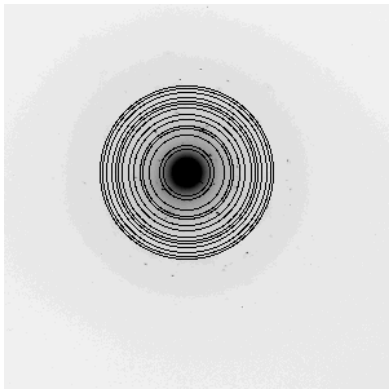	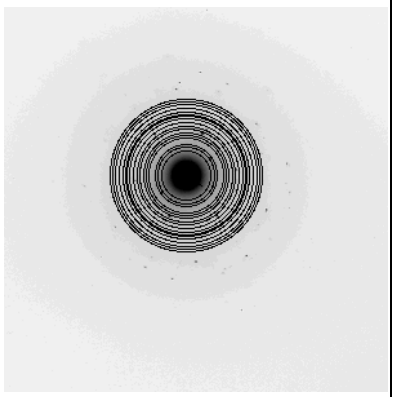	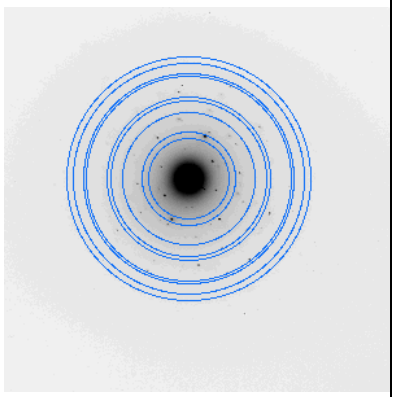
S622	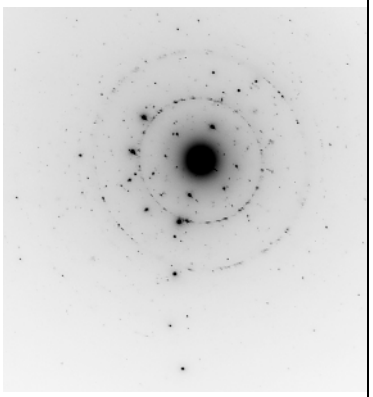	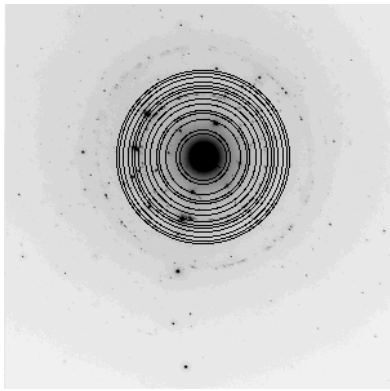	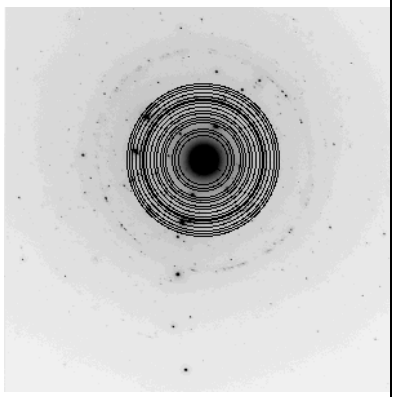	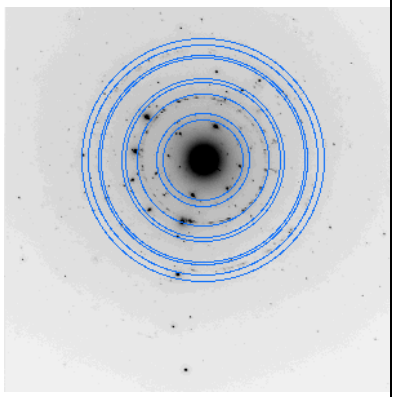

S623	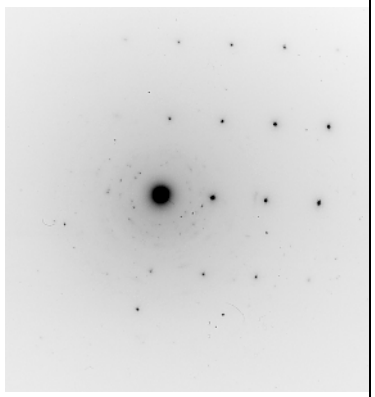	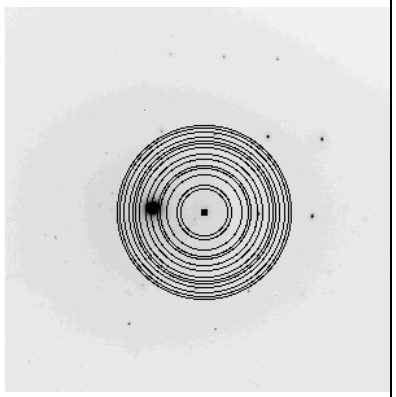	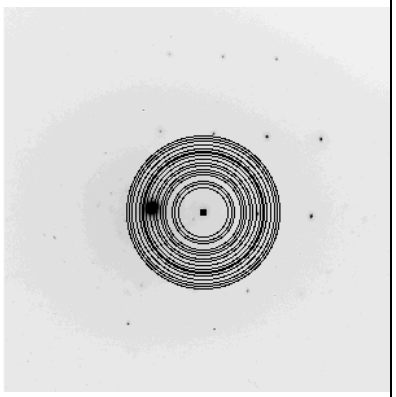	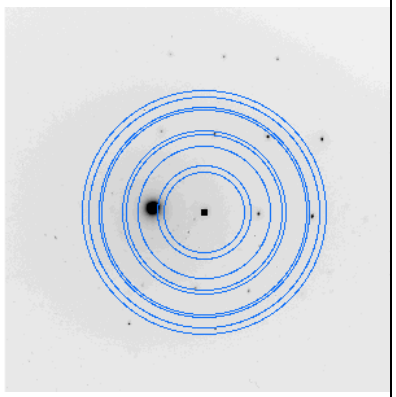
S626	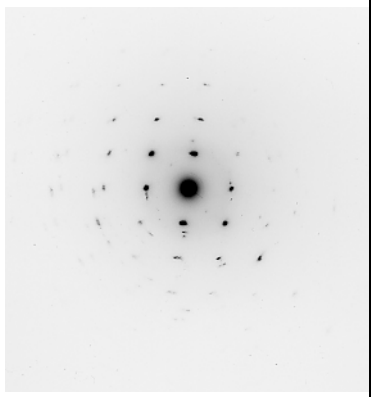	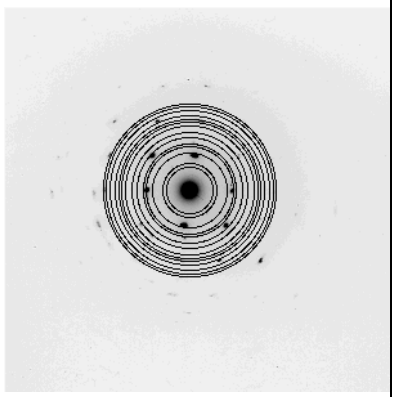	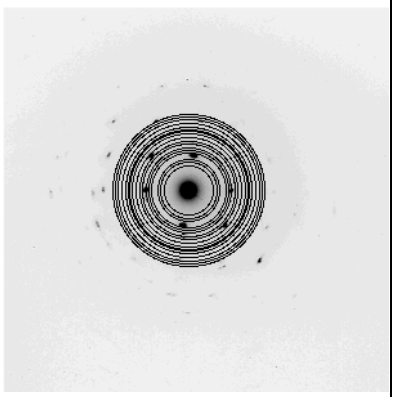	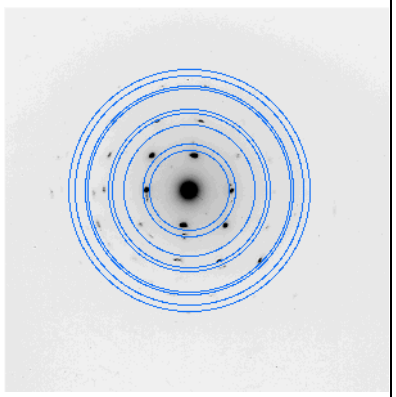

Table 1. Summary of drill holes sampled for mineralogy sub-project 7. This is a subset of the drill holes logged for stratigraphy and sedimentology in the eastern Athabasca Basin, EXTECH IV (after Jefferson et al., 2001).

DDH #	Company	UTM_E_ Nad 83	UTM_N_ Nad 83	Disposition	Collar (m)	MF Sub-unit thickness (m)				U/C (m)	Notes/person-date logged
						MFd	MFc	MFb	Mfa(?)		
Close Lake Transect											
CLC10-76	COGEMA	500125	6419911	S101497		154	123	301**		585	Jefferson quick log 2000
CLC10-77	COGEMA	499710	6420061	S104781		145	243	170	93.42	602.8	Jefferson 2000
MAC-186	Cameco	514985	6406109	S105657	520	180	46	189*		443.4	industry * Mfa/MFb & fanglomerate
MAC-189	Cameco	509543	6407636	S101722	502	146	72	188*		411.6	industry * Mfa/MFb & fanglomerate
McArthur River Transect											
CLC1-047	COGEMA	492800	6415586		558	303.1	79	213	58.88	672.88	Jefferson 2001
CLC1-049	COGEMA	493750	6415711		547	243	44	225	75.9	591.9	Jefferson 2001
MAC-061	SMDC	507546	6379615	ML5298	518	0	37	112		191.1	Industry
MAC-100	Cameco	499717	6395936	S105665	545	69	98	115	98	381	Jefferson 2000
MAC-107	Cameco	499663	6396844	S105665	550	94.5	140	86.6	70.1	391.1	Industry
MAC-107	Cameco	499663	6396844	S105665	550	94.5	140	123	34.1	391.1	Jefferson 2000
MAC-111	Cameco	500144	6395326	S105665	537.9	106	95	117	92	410.8	Jefferson 2000
MAC-111	Cameco	500144	6395326	S105665	537.9	106	95	150	59.5	410.8	Jefferson 2000
MAC-198	Cameco	497350	6402590		542	182	37	195	58	485	Bernier 2002
MAC-224*	Cameco	496455	6401577		536.8	197	79	175	64	513.5	Williamson 2000; Jefferson & Collier 2001
RL-046	Cameco	495345	6403030		560	171	55	141	117.5	555.5	Bernier 2001
RL-063	Cameco	496250	6401761		535	199	93	139	131	566	Group of six 2001
RL-064**	Cameco	496811	6402576		554	191	78	116	124	531	Group of six 2002
RL-068	Cameco	496200	6401661		535	190.55	75	180	80	580.5	Group of six 2001
RL-099	Cameco	489797	6398985	CBS 8926	580	124	165	66	65	431.5	Jefferson 2000 picks with McHardy

Thicknesses of Manitou Falls Formation subunits in metres are provided to exemplify regional trends. Some data are from company logs. Basal units of MAC-186 and 189 include MFa, MFb, and paleo-talus deposits colloquially termed "fanglomerate". Basal units of CLC10-77 include COGEMA subunits MFb1 to 4.
*also logged by Hiatt and Kyser (2007)
** re-interpreted by Ramaekers et al. (2007)

Table 2: Normalized (wt%) TEM-EDS analyses. Four areas were examined and spectra were collected on different spots of sample 01JP27a. Results organized based on mineral variety determined (right-hand column: APS= Alumino-phosphate mineral; Th=Thorium; Sr=Strontium; Mnz=Monazite; Qtz=Quartz; Kfs=K-Feldspar; Mca=Mica; Rt=Rutile; Zrn=Zircon; Xtm=Xenotime).

Sample No.	O	Si	Ti	Al	Fe	Mg	Ca	K	P	S	Ba	Cu	Sr	Th	Zr	Total	Mineral
Spect 4-6	21.02	1.30	1.85	21.82	0.46	0.00	2.69	0.84	12.25	3.46	1.95	16.39	15.97	0.00	0.00	100	APS-no Th
Spect 4-8	40.03	2.62	0.00	17.94	0.37	0.00	2.06	1.03	9.51	2.77	1.05	9.96	11.37	0.00	1.29	100	APS-no Th
Spect 4-9	40.97	0.75	0.00	16.91	0.15	0.00	1.85	0.33	10.26	2.42	1.79	11.10	13.45	0.00	0.00	100	APS-no Th
Spect 4-11	26.59	0.00	0.00	24.16	0.11	0.00	1.91	0.00	14.06	5.98	0.54	7.01	18.34	0.00	1.31	100	APS-no Th
Spect 1-2	41.16	2.90	0.00	11.97	0.69	0.00	1.08	0.17	10.21	1.24	0.69	10.91	5.42	2.13	11.45	100	APS
Spect 1-5	35.13	0.00	0.00	15.66	2.02	0.00	2.30	0.00	9.43	1.27	1.62	14.99	10.41	7.17	0.00	100	APS
Spect 1-6	44.76	0.00	0.00	15.10	1.50	0.00	2.05	0.00	8.59	1.67	1.47	11.19	9.82	3.85	0.00	100	APS
Spect 1-7	24.67	0.00	0.00	18.11	2.46	0.00	2.37	0.00	9.65	2.23	1.90	21.06	11.69	5.88	0.00	100	APS
Spect 1-9	39.53	1.15	0.00	13.34	0.79	0.00	1.48	0.00	8.38	0.87	1.37	18.60	6.35	3.86	4.29	100	APS
Spect 1-17	36.13	0.35	0.00	16.45	2.63	0.00	1.95	0.12	9.94	2.01	1.45	11.93	10.24	6.06	0.75	100	APS
Spect 1-18	43.80	0.36	0.00	16.35	1.14	0.00	1.68	0.00	8.82	2.44	0.71	11.99	10.45	2.27	0.00	100	APS
Spect 1-23	29.04	0.44	0.39	17.70	3.21	0.00	2.70	0.00	10.18	1.72	1.60	13.54	10.46	7.02	2.01	100	APS
Spect 1-24	27.36	0.55	0.00	17.80	3.09	0.00	2.50	0.00	10.78	1.60	1.52	13.77	9.59	8.93	2.50	100	APS
Spect 1-26	15.18	0.87	0.00	17.95	3.81	0.00	3.10	0.14	11.23	2.77	1.65	21.52	11.56	6.44	3.80	100	APS
Spect 1-28	37.09	0.93	0.62	15.85	1.14	0.00	1.84	0.00	9.80	1.47	1.64	15.90	9.41	3.01	1.31	100	APS
Spect 1-30	42.26	0.53	0.00	14.71	1.84	0.00	1.74	0.00	8.95	2.61	1.17	12.53	8.35	2.89	2.44	100	APS
Spect 1-31	43.71	0.31	0.00	14.26	1.17	0.00	1.88	0.11	10.35	1.10	2.15	12.65	6.82	5.50	0.00	100	APS
Spect 1-33	41.93	0.43	0.00	15.25	0.83	0.00	1.61	0.00	9.83	1.00	2.22	15.92	7.99	3.00	0.00	100	APS
Spect 1-34	35.51	0.87	0.00	16.31	1.54	0.00	2.10	0.00	11.24	2.40	0.00	17.25	8.50	4.29	0.00	100	APS
Spect 1-35	47.58	0.00	0.00	14.20	1.49	0.00	1.95	0.00	9.00	1.73	0.00	13.83	7.94	2.27	0.00	100	APS
Spect 1-36	44.77	0.00	0.00	13.86	1.50	0.00	1.32	0.00	9.51	1.61	1.12	15.53	7.12	3.67	0.00	100	APS
Spect 1-38	39.87	0.90	0.00	11.85	0.80	0.00	1.00	0.00	9.04	0.91	0.00	26.90	6.59	2.14	0.00	100	APS
Spect 1-39	39.33	0.00	0.00	14.67	2.06	0.00	1.83	0.00	9.00	1.50	1.39	17.58	8.76	3.89	0.00	100	APS
Spect 1-40	32.66	0.00	0.00	14.23	0.97	0.00	1.24	0.00	11.66	1.42	0.00	26.87	7.47	3.48	0.00	100	APS
Spect 2-2	8.76	1.07	0.00	17.43	3.48	0.00	3.91	0.00	11.86	2.01	1.35	26.08	11.93	7.10	5.05	100	APS

Table 2: Continued.

Sample No.	O	Si	Ti	Al	Fe	Mg	Ca	K	P	S	Ba	Cu	Sr	Th	Zr	Total	Mineral
Spect 3-1	39.41	0.00	0.00	13.57	1.59	0.00	1.51	0.00	7.77	1.63	1.04	22.25	8.22	3.02	0.00	100	APS
Spect 3-3	35.96	0.30	0.00	14.80	1.99	0.00	1.61	0.00	8.26	1.20	1.20	18.75	8.26	5.95	1.73	100	APS
Spect 3-4	30.09	2.62	0.00	16.17	1.63	0.00	1.34	0.48	8.24	1.83	0.00	25.31	6.09	4.86	1.35	100	APS
Spect 3-8	31.79	0.00	0.00	14.31	1.34	0.00	1.44	0.00	8.98	1.66	0.00	29.93	6.86	3.69	0.00	100	APS
Spect 3-9	39.49	0.82	0.00	10.20	0.93	0.00	0.95	0.00	9.73	1.25	0.74	24.63	5.57	3.09	2.60	100	APS
Spect 3-10	38.67	2.51	0.00	14.69	1.36	0.00	0.91	0.14	10.47	1.07	0.68	19.51	4.99	3.15	1.85	100	APS
Spect 3-11	36.56	0.00	0.00	12.95	1.09	0.00	1.08	0.00	11.79	1.69	0.61	23.28	5.84	3.26	1.86	100	APS
Spect 3-12	41.11	0.56	0.00	12.81	1.10	0.00	1.35	0.00	7.89	1.36	0.73	21.28	6.46	3.14	2.22	100	APS
Spect 3-13	40.15	0.33	0.00	15.06	1.07	0.00	1.36	0.00	8.08	2.40	0.73	15.31	8.32	1.88	5.33	100	APS
Spect 3-14	37.63	0.79	0.00	13.88	1.33	0.00	1.58	0.00	10.01	1.80	1.18	18.26	7.12	4.00	2.44	100	APS
Spect 3-15	38.02	2.77	0.00	12.60	0.86	0.00	1.01	0.14	8.19	1.28	0.43	19.10	5.28	2.98	7.35	100	APS
Spect 4-1	30.96	0.91	0.18	22.54	0.82	0.00	1.70	0.00	11.13	0.00	1.34	16.24	13.19	1.00	0.00	100	APS
Spect 4-2	25.41	2.91	0.36	24.87	0.69	0.00	2.13	0.00	8.50	0.00	1.40	16.02	17.18	0.53	0.00	100	APS
Spect 4-3	27.04	2.81	0.00	20.44	1.08	0.00	2.54	0.41	7.36	0.16	1.24	18.93	16.03	1.95	0.00	100	APS
Spect 4-4	23.39	1.96	0.00	19.49	1.21	0.00	3.34	0.00	8.02	0.21	1.52	18.51	20.74	1.61	0.00	100	APS
Spect 4-7	22.28	0.46	1.13	21.31	0.61	0.00	2.44	0.39	12.10	3.69	1.54	13.08	17.94	0.82	2.21	100	APS
Spect 4-10	40.33	0.77	0.21	16.10	0.56	0.00	2.05	0.17	11.52	1.09	5.22	7.31	9.44	1.31	3.93	100	APS
Spect 1-3	14.88	7.98	0.00	2.92	0.99	0.00	1.22	0.00	2.96	0.00	0.00	25.71	0.00	4.68	38.65	100	APS-no Sr (mnz?)
Spect 1-4	40.60	2.17	0.00	17.34	1.78	0.26	2.15	0.25	9.52	1.78	1.09	8.26	9.17	3.74	1.91	100	APS/Mca
Spect 1-25	40.22	0.83	0.00	16.01	1.02	0.12	1.41	0.10	8.54	2.71	0.88	11.17	10.17	3.11	3.72	100	APS/Mca
Spect 1-27	30.21	0.87	0.00	17.48	4.17	0.20	2.08	0.13	9.90	1.52	1.38	14.27	9.91	6.19	1.68	100	APS/Mca
Spect 1-32	39.19	0.41	0.00	16.15	2.17	0.17	2.09	0.00	10.25	1.93	1.51	11.49	8.84	4.55	1.25	100	APS/Mca
																	APS/Mca
Spect 2-1	20.58	0.72	0.00	16.53	2.90	0.37	2.85	0.00	9.30	1.33	1.28	20.75	10.54	7.65	5.23	100	APS/Mca
																	APS/Mca
Spect 3-2	42.61	4.04	0.00	15.01	1.07	0.45	1.44	0.53	7.06	1.56	0.96	16.19	6.04	3.05	0.00	100	APS/Mca
Spect 3-7	43.80	0.40	0.00	13.17	0.64	0.22	1.40	0.00	8.54	1.95	0.67	20.52	6.03	2.67	0.00	100	APS/Mca

Table 2: Continued

Sample No.	O	Si	Ti	Al	Fe	Mg	Ca	K	P	S	Ba	Cu	Sr	Th	Zr	Total	Mineral
Spect 1-1	45.47	44.19	0.00	0.00	0.00	0.00	0.00	0.00	0.00	0.00	0.00	10.34	0.00	0.00	0.00	100	Qtz
Spect 1-21	50.23	42.56	1.87	0.00	0.16	0.00	0.00	0.00	0.00	0.00	0.00	5.19	0.00	0.00	0.00	100	Qtz
Spect 1-29	45.31	36.12	0.00	3.40	0.00	0.00	0.35	0.20	0.00	0.00	1.75	12.87	0.00	0.00	0.00	100	Qtz/Kfs
Spect 1-10	40.51	26.14	0.00	5.35	0.00	0.63	0.44	1.33	0.00	0.39	0.00	25.21	0.00	0.00	0.00	100	Mca
Spect 1-11	26.18	10.20	0.00	10.07	0.35	2.60	0.00	1.05	0.00	0.00	0.00	49.55	0.00	0.00	0.00	100	Mca
Spect 1-12	44.91	28.12	0.00	3.58	0.00	0.51	0.43	0.88	0.00	0.22	1.07	20.28	0.00	0.00	0.00	100	Mca
Spect 1-14	44.20	27.31	0.00	5.67	0.20	0.83	0.19	0.64	0.00	0.00	0.00	20.98	0.00	0.00	0.00	100	Mca
Spect 1-15	27.81	11.30	0.00	10.39	0.37	1.69	0.00	1.88	0.00	0.00	0.00	46.56	0.00	0.00	0.00	100	Mca
Spect 1-16	17.85	7.54	0.00	6.57	0.00	1.78	0.00	1.07	0.00	0.00	0.00	65.19	0.00	0.00	0.00	100	Mca
Spect 1-22	49.41	34.08	0.00	3.29	0.14	0.38	0.33	1.08	0.00	0.10	1.66	9.54	0.00	0.00	0.00	100	Mca
Spect 1-37	40.83	17.92	0.00	16.53	0.00	0.97	0.00	0.85	0.00	0.00	0.00	22.90	0.00	0.00	0.00	100	Mca
Spect 3-5	40.41	17.65	0.00	14.79	0.79	1.03	0.00	4.42	0.00	0.00	0.00	20.92	0.00	0.00	0.00	100	Mca
Spect 3-6	37.00	18.53	0.00	16.21	0.69	0.83	0.00	4.94	0.00	0.00	0.00	21.80	0.00	0.00	0.00	100	Mca
Spect 1-13	37.23	4.28	31.59	3.07	1.94	0.27	0.12	0.91	0.39	0.00	0.00	18.38	0.00	0.00	1.82	100	Rt/Mica
Spect 1-19	35.40	0.43	47.71	0.37	2.20	0.00	0.00	0.00	0.00	0.00	1.18	12.72	0.00	0.00	0.00	100	Rt
Spect 1-20	37.59	0.65	39.70	0.21	1.54	0.00	0.15	0.00	0.00	0.00	0.00	17.55	0.00	0.00	2.61	100	Rt
Spect 4-5	41.49	0.58	39.83	0.00	0.79	0.00	0.00	0.00	0.00	0.00	0.00	17.30	0.00	0.00	0.00	100	Rt
Spect 1-8	32.36	3.75	0.00	7.21	0.00	0.00	1.32	0.00	3.85	0.00	0.00	32.81	0.00	0.00	18.71	100	Zrn or Xtm